ESR Studies of Spin-Labeled Membranes Aligned by Isopotential Spin-Dry Ultracentrifugation: Lipid-Protein Interactions

Mingtao Ge, David E. Budil, and Jack H. Freed
Baker Laboratory of Chemistry, Cornell University, Ithaca, New York 14853 USA

ABSTRACT Electron spin resonance (ESR) studies have been performed on spin-labeled model membranes aligned using the isopotential spin-dry ultracentrifugation (ISDU) method of Clark and Rothschild. This method relies on sedimentation of the membrane fragments onto a gravitational isopotential surface with simultaneous evaporation of the solvent in a vacuum ultracentrifuge to promote alignment. The degree of alignment obtainable using ISDU, as monitored by ESR measurements of molecular ordering for both lipid (16-PC) and cholestane spin labels (CSL), in dipalmitoylphosphatidylcholine (DPPC) model membranes compares favorably with that obtainable by pressure-annealing. The much gentler conditions under which membranes may be aligned by ISDU greatly extends the range of macroscopically aligned membrane samples that may be investigated by ESR. We report the first ESR study of an integral membrane protein, bacteriorhodopsin (BR) in well-aligned multilayers. We have also examined ISDU-aligned DPPC multilayers incorporating a short peptide gramicidin A′ (GA), with higher water content than previously studied. 0.24 mol % BR/DPPC membranes with CSL probe show two distinct components, primarily in the gel phase, which can be attributed to bulk and boundary regions of the bilayer. The boundary regions show sharply decreased molecular ordering and spectral effects comparable to those observed from 2 mol % GA/DPPC membranes. The boundary regions for both BR and GA also exhibit increased fluidity as monitored by the rotational diffusion rates. The high water content of the GA/DPPC membranes reduces the disordering effect as evidenced by the reduced populations of the disordered components. The ESR spectra obtained slightly below the main phase transition of DPPC from both the peptide- and protein-containing membranes reveals a new component with increased ordering of the lipids associated with the peptide or protein. This increase coincides with a broad endothermic peak in the DSC, suggesting a disaggregation of both the peptide and the protein before the main phase transition of the lipid. Detailed simulations of the multicomponent ESR spectra have been performed by the latest nonlinear least-squares methods, which have helped to clarify the spectral interpretations. It is found that the simulations of ESR spectra from CSL in the gel phase for all the lipid membranes studied could be significantly improved by utilizing a model with CSL molecules existing as both hydrogen-bonded to the bilayer interface and non-hydrogen-bonded within the bilayer.

INTRODUCTION

Electron spin resonance (ESR) studies of spin-labeled membranes have been very important in the study of membrane structure (Hubbell and McConnell, 1971; Tanaka and Freed, 1984; Kar et al., 1985), of fluidity (Marsh, 1980), and of thermodynamics (Shin and Freed, 1989a, b; Shin et al., 1993), as well as the nature of lipid-protein interactions within the membrane (Jost et al., 1973a; Marsh and Watts, 1981; Tanaka and Freed, 1985; Ge and Freed, 1993). However, the information obtainable from direct study of naturally occurring membranes by ESR is frequently limited by a lack of resolution owing to the fact that such systems are often only available as randomly oriented membrane dispersions. For this reason, many spin-label studies have focused on model membrane systems, which have the advantage that they can be macroscopically aligned with very high ordering. This greatly enhances the resolution with which the membrane can be studied, providing detailed information on lipid chain mobility and ordering that would be difficult or impossible to obtain from dispersion samples by conventional ESR.

Unfortunately, the procedures which generally give the best alignment for model membranes, such as pressure-annealing (Powers and Clark, 1975; Powers and Pershan, 1977; Shimoyama et al., 1978; Koole et al., 1984; Tanaka and Freed, 1984, 1985; Kar et al., 1985; Shin and Freed, 1989a, b; Ge et al., 1994) are too rigorous to permit the incorporation of integral proteins, and they have not been applied successfully to naturally occurring membranes. The major obstacles to applying pressure-annealing to either natural membranes or reconstituted systems are 1) the prolonged exposure to the higher temperatures required for annealing the membrane (about 20°C above the main transition temperature of the lipid), and 2) the use of organic solvents to deposit the membranes (Powers and Pershan, 1977; Tanaka and Freed, 1984, 1985; Shin and Freed, 1989a), both of which may destroy labile membrane components. Moreover, pressure-annealing even fails to align model membranes when they contain a high concentration of a small peptide; e.g., for concentrations of the peptide gramicidin A (GA) greater than 4 mol % (Tanaka and Freed, 1985).

In contrast, there are several alignment methods that are gentle enough for labile membrane components, including 1) drying of lipid membranes containing an integral protein (Jost et al., 1973b) or a peptide (Vogel et al., 1983), 2) membrane

Received for publication 9 November 1993 and in final form 16 September 1994.

Address reprint requests to Dr. Jack H. Freed, Department of Chemistry, Cornell University, B52 Baker Laboratory, Ithaca, NY 14853-1301. Tel.: 607-255-3647; Fax: 607-255-4137.

0006-3495/94/12/2326/19 $2.00

deposition by ultracentrifugation (Herbette et al., 1977), and 3) alignment in a strong magnetic field (Frank et al., 1979). However, these methods suffer the significant drawback that they can give only a partial alignment, thus limiting the resolution with which the membranes can be studied by ESR.

Clark and Rothschild (1982) introduced the method of isopotential spin-dry ultracentrifugation (ISDU) for aligning membranes from an aqueous suspension of vesicles or membrane fragments. Briefly, ISDU requires sedimentation of vesicles or membrane fragments onto a gravitationally isopotential surface by ultracentrifugation, with simultaneous evaporation of the solvent (water) under vacuum. The method is based on a detailed analysis carried out by Clark et al. (1980) that considered such factors as membrane fragment size, steric interactions, bilayer elasticity, and thermal fluctuations. These workers found that, whereas centrifugation promotes bilayer order by allowing a layer-by-layer deposition of membrane fragments onto an aligning surface, the available gravitational fields are insufficient to overcome the disorienting influences of the intrinsic curvature of closed membrane structures as well as the thermal fluctuations in the membrane curvature. In contrast, while the capillary forces due to water evaporation are high enough to collapse curved membranes, as evaporation proceeds, the concentrated membrane fragments aggregate into larger groups that are less sensitive to the orienting influence of the surface, leading to incomplete alignment of the fragments. Based on their analysis, Clark et al. (1980) proposed that the combination of ultracentrifugation and drying should produce significantly better membrane alignment than that achievable by either method alone. Clark, Rothschild, and co-workers were able to demonstrate and characterize the exceptionally high alignment of purple and photoreceptor membranes produced by their combined method using direct observation by freeze-fracture electron microscopy (Clark et al., 1980), optical spectroscopy (Rothschild and Clark, 1980; Rothschild et al., 1980), and x-ray diffraction (Clark and Rothschild, 1982).

Although ISDU has not previously been utilized in spin-label studies, it is particularly attractive for this method because it can be applied to naturally occurring membranes as well as lipid vesicles, into which a wide variety of proteins may be reconstituted (Clark and Rothschild, 1982). Given the major role that ESR has played in studies of membrane structure and dynamics, ISDU would appear to be a promising means of extending the high-resolution ESR methods that have been successfully applied to model membranes to a much wider range of membrane systems with more direct biological relevance.

In this work we clearly demonstrate the value of ISDU for ESR studies. We first present an evaluation of ISDU using the ESR spin-label method. To make a comparison with other alignment techniques, we chose initially to investigate several systems that are similar to those previously studied by ESR using pressure-annealing (Tanaka and Freed, 1984, 1985; Kar et al., 1985; Shin and Freed, 1989a). Specifically, we studied membranes of pure dipalmitoylphosphatidylcholine (DPPC) and DPPC membranes containing a short peptide, gramicidin A′. Our initial objective was to assess the relative degree of membrane alignment afforded by the two methods as monitored by ESR. In general, we find that ISDU compares favorably with pressure-annealing as an alignment method for ESR work, i.e., ISDU-aligned membranes are highly ordered in both gel and liquid crystalline phases, affording information about ordering and fluidity with the same degree of resolution and accuracy. We did take advantage of the flexibility of the ISDU method for preparing substantially hydrated samples to study samples with higher water content (20 wt % water) compared with previous studies on low water content samples (4–7 wt %). This enabled us to confirm that the general trend in the effect of GA on the ordering and dynamics of the membrane were very similar despite the differences in water content.

After establishing the suitability of the ISDU method for high-resolution spin-label studies, we demonstrate its applicability for aligning membranes reconstituted with an integral membrane protein, specifically bacteriorhodopsin (BR). For the membranes reconstituted with either BR or GA, the high resolution of the ESR spectra from the aligned samples have led to new observations. That is, the ESR spectra reveal a significant increase in the ordering of lipids associated with the BR or GA that correlates well with an endothermic enthalpy change observed by differential scanning calorimetry (DSC) at temperatures somewhat below the main gel-to-liquid crystal phase transition of the lipid. These effects may be associated with disaggregation of the protein upon warming before the main phase transition. Our results suggest that spin-label studies of aligned membranes are quite sensitive to protein-protein interactions within the membrane.

This work also features several advances in the methods of slow-motional ESR spectral simulation used in the experimental analysis, as compared with previous spin-label studies of aligned membranes (Kar, 1985; Tanaka and Freed, 1984, 1985; Shin and Freed, 1989a, b). Recent improvements in the efficiency of ESR line shape calculations and in the least-squares algorithm used to fit the experimental spectra have made it possible to carry out a single global fit to a series of spectra with differing membrane orientations relative to the magnetic field, wherein each such spectrum may exhibit a number of components having different ordering and motion properties. Such a capability has proved particularly useful for studying aligned, peptide- and protein-containing membranes, which frequently exhibit more than one spectral component. This was essential for the analysis of the protein and peptide disaggregation effects mentioned above. It has also led to new analysis of the ESR spectra of cholestane spin label (CSL) in DPPC/GA and DPPC/BR systems, as well as in pure DPPC membranes; i.e., in the gel phase of all the DPPC membranes studied in this work, we distinguish a "hydrogen-bonded" CSL species that undergoes faster rotational diffusion than a "non-hydrogen-bonded" CSL species, that is also observed.

These ESR spectral simulation methods provide a powerful alternative to the commonly used spectral subtraction methods (Marsh and Watts, 1981) in the study of protein-lipid interactions. By the simulation method a quantitative

interpretation of the components in terms of their ordering and dynamics is achieved, as well as their relative populations. Subtraction methods can only provide the latter. For subtraction methods to be effective, one must have a good reference spectrum to subtract, and this is not necessarily the case (e.g., the "hydrogen-bonded" versus "non-hydrogen bonded" CSL species described in this work). Furthermore, the reference component could change its spectral properties with changes in temperature, composition, etc. (e.g., the bulk lipid phase could be modified as protein is added) leading to uncertainties in spectral subtraction. Simulation methods do not have these limitations. One should also note that the justification for spectral subtraction is not always clear from just the appearance of the spectrum, but simulation methods can help to clarify whether a single component is adequate to fit the observed spectrum (Meirovitch et al., 1984). However, simulation methods do rely on having satisfactory dynamic models to fit the component spectra. The fits we achieve in the present work, as well as in previous studies (Ge and Freed, 1993; Ge et al., 1994; Meirovitch et al., 1984; Kar et al., 1985; Shin and Freed, 1989a, b; Tanaka and Freed, 1984, 1985), indicate that the dynamic models are satisfactory.

MATERIALS AND METHODS

Isopotential spin-dry ultracentrifugation

We used a modification of the method outlined by Clark and Rothschild (Clark et al., 1980; Clark and Rothschild, 1982) to carry out the isopotential spin-dry procedure. The major difference between their method and the one described below is in the construction of the isopotential ultracentrifuge cells. Because the Beckman SW-27 swinging-bucket rotor used for our experiments is shared with several other research groups, we were unable to modify the rotor buckets permanently as described (Clark and Rothschild, 1982). Instead, our ISDU cell was constructed to fit inside a removable polycarbonate centrifuge tube. The bottom of the tube was filled with a machinable epoxy and machined to a flat surface located 12 mm from the bottom of the tube.

Fig. 1 shows a diagram of the ISDU cell used in this work. The body of the cell consists of a black delrin base, a thin stainless steel plug, and a reservoir, also fabricated from black delrin, which are fastened together with four long screws. The side of the steel plug toward the sample and the bottom of the delrin reservoir piece are machined to a cylindrical surface with radius equal to the distance of the surface from the center of rotation. For accurate alignment of the axis of the isopotential surface with respect to the rotation axis, an alignment pin was placed in the bottom of the base which fit into a small hole drilled into the epoxy fill. A reference notch corresponding to the location of the alignment hole was machined into the rim of each polycarbonate tube to allow alignment of the tube with respect to the rotor bucket. The tubes were wrapped with a layer of Teflon tape to prevent misalignment during rotor acceleration.

To allow for sample drying, the centrifugation was carried out with a small (2–5 mm) gap in the O-ring that is used to seal the bucket cap, instead of drilling a hole into the bucket cap. For better control of the evaporation rate, a pinhole (Melles Griot) mounted on a thin stainless steel washer was fixed on top of the reservoir using a screw plug and an O-ring. We utilized a range of pinhole sizes from 100 to 400 μm to control the evaporation rate.

The aligned membranes were deposited on No. 1 thickness glass microscope coverslips that had been cut to the proper size (~12 × 12 mm) with a diamond stylus; alternatively, commercially available circular coverslips 10 mm in diameter also worked quite well. Before use, the coverslips were cleaned with hot concentrated sulfuric acid and rinsed extensively with

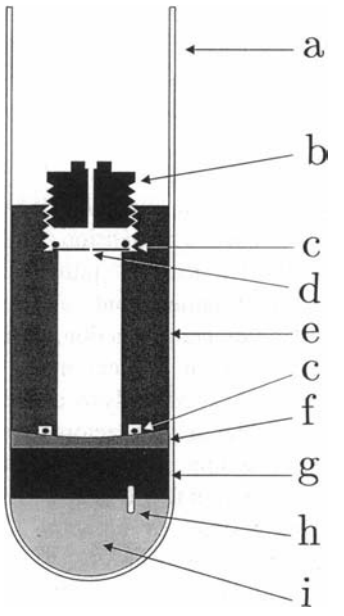

FIGURE 1 Diagram of the ISDU cell. (*a*) Polycarbonate tube (Beckmann); (*b*) screw cap; (*c*) O-ring seals; (*d*) pinhole; (*e*) cell reservoir body (made from delrin); (*f*) stainless steel plate with isopotential surface; (*g*) delrin support plug; (*h*) placement pin; (*i*) epoxy fill.

methylene chloride or chloroform. A clean coverslip was inserted into the centrifugation cell and clamped between the cell reservoir and the isopotential surface with an O-ring seal. Up to ~1 ml of a vesicle suspension was introduced into the cell, the cell sealed with the screw plug, and the suspension ultracentrifuged for up to 20 h at 25°C and 15,000–17,000 rpm, which resulted in samples with at least 10% water.

Preparation of vesicles

DPPC was purchased from Avanti Polar Lipids, Inc. (Birmingham, AL) and was used without any further purification. The 3-doxyl CSL was purchased from Syva Co. (Palo Alto, CA) and recrystallized from ethanol. To prepare unilamellar vesicles (ULV), measured amounts of lipid and spin label were suspended in deionized water and then sonicated at a power of 3 W for <10 min at 55°C, which is above the main phase transition of DPPC. Approximately 10 mg of lipid was used per ml of water. The lipids were weighed directly and the spin labels measured by evaporating a known volume of a stock solution in chloroform to give a concentration of 0.5 mol % in all samples studied. Upon formation of ULV by sonication, which is not only necessary for best alignment of the membranes by ISDU, but is also required for the incorporation of BR (see below), the milky white suspension became nearly clear and opalescent. The integrity of the lipid during sonication was verified by comparing thin-layer chromatographs of the starting material and the vesicle suspension. After formation of ULV, the suspension was spun in a benchtop lab centrifuge for 0.5 h to remove any metal particles from the sonicator horn that may be present before aligning by ISDU.

Incorporation of GA

GA was obtained from Sigma Chemical Co. (St. Louis, MO) and used without further purification. For incorporation into the vesicles, weighed amounts of the peptide were dissolved in methanol and mixed with the DPPC chloroform solution before the solvent evaporation and sonication steps described above.

Incorporation of BR

BR used in this study was the kind gift of Dr. Anthony Scotto of the Cornell Medical College. For incorporation of BR into the lipid vesicles, the BR was

added after the initial formation of the ULV either in the form of lyophilized protein, or as a detergent-free suspension in deionized water. The protein was then incubated with the vesicles at 65°C (well below the denaturation temperature of BR, as discussed below) for 12 h and sonicated in 1-min bursts repeated every hour. There was no change in the integrity of the protein during this process as monitored by ultraviolet/visible absorption spectroscopy (cf. Discussion). In addition, sucrose density gradient ultracentrifugation (Casadio and Stoeckenius, 1980) produced a single colored band, indicating that the BR was incorporated into the vesicles.

It should be emphasized that the incubation temperature of 65°C used to incorporate the BR into the DPPC vesicles for the present study is not a necessary feature of the ISDU procedure. In fact, the spin-dry step itself took place near 20°C and can easily be carried out at lower temperatures to accommodate proteins or membranes that are more heat-labile than BR/DPPC. The 65°C incubation for the present study was determined by the relatively high gel-to-liquid crystal transition of DPPC (41°C in excess water), which was utilized to enable a direct comparison of BR-containing membranes with previous studies of pure and GA-containing DPPC membranes aligned by pressure annealing, and because of the known high thermal stability of BR. In general, incubation can be performed several degrees above the main transition (e.g., 30°C for DMPC).

ESR sample preparation

After ultracentrifugation, the membranes were removed from the cell and their alignment at the center was immediately checked using a polarizing microscope (Nikon, Inc., Instrument Division, Garden City, NJ). Any samples that did not exhibit the distinctive interference pattern indicative of an aligned sample were immediately discarded. If necessary, the more poorly aligned edges of the sample were carefully removed with a sharp razor blade and the samples immediately inspected for damage (Kar et al., 1985). About 50% of the samples were usable at this stage; the major reasons for discarding a sample include 1) trapped bubbles within the deposited membrane layer, 2) fracture of the glass plate during ultracentrifugation, 3) failure to complete the spin-drying process, and 4) rough surface of the sample.

The aligned membranes (with or without GA and BR) were typically 50–100 μm in thickness, although significantly thicker samples could be prepared (up to 400 μm). For ESR temperature studies, the aligned membrane was covered with a second clean glass plate and placed into a sealed container containing a reservoir of deionized water for hydration for more than 48 h. The pure DPPC membrane hydrated in this manner contained 20 wt % water by weight. We found that further hydration did not increase water content any further, i.e., equilibrium was reached. After hydration, the sample was wrapped with thin Teflon tape and the entire sample was sandwiched between two sheets of Mylar and its edges sealed with epoxy. For the usable samples, we found <5% defects from the ESR spectra. This residual amount of defect is found to be primarily due to edge effects in the ISDU samples.

ESR spectroscopy and spectral analysis

Spectra were obtained on a Bruker Instruments ER-200 ESR spectrometer at a frequency of 9.55 GHz under standard conditions (Kar et al., 1985; Tanaka and Freed, 1984, 1985; Shin and Freed, 1989a). The field sweeps were calibrated with a Bruker ER 035 M NMR gaussmeter. All spectra were digitized to 1024 points and had approximately 100G sweep widths. Typically spectra were measured for both $\Psi = 0°$ and $\Psi = 90°$, where Ψ is the tilt angle of the multilayer normal relative to the dc magnetic field. Spectra were analyzed to obtain the ordering and rotational dynamics utilizing ESR spectral simulation methods based on the stochastic Liouville equation (Meirovitch et al., 1982; Schneider and Freed, 1989). The simulations were fit to the experimental data for both 0° and 90° tilt angles simultaneously, utilizing a modified Levenberg-Marquardt nonlinear least square minimization algorithm (Dennis and Schnabel, 1983; More et al., 1980) to obtain the optimum ESR parameters (Crepeau et al., 1987; Shin and Freed, 1989).

For least-squares fits involving more than one spectral component, the relative amounts of the individual components were obtained using a "separable least-squares" procedure in which the scaling factors for each component were optimized separately from the nonlinear fitting parameters at each iteration of the nonlinear parameter minimization. The scaling factors were determined by a linear least-squares procedure utilizing the component spectra calculated from the nonlinear fitting parameters (Seber and Wild, 1989). For fits of spectra from more than one tilt angle, the scaling factors were determined globally for the set after normalizing the integrated intensity of each spectrum. The linear least squares was carried out using the standard QR factorization method (Dongarra et al., 1979). The diagonal elements of the R matrix factor provide a quantitative criterion for determining the number of spectral components that are sufficiently resolvable (i.e., linearly independent) within a given experimental signal-to-noise ratio (Dongarra et al., 1979). Estimates of nonlinear parameter uncertainties and uniqueness-of-fit (i.e., the degree of correlation between parameters) were obtained by calculating the parameter covariance matrix from the curvature matrix utilized in the Levenberg-Marquardt algorithm under the standard "linearization" approximation (Seber and Wild, 1989). The linear least-squares factorization and the correlation matrix generally provided good indications of the maximum number of spectral components and fitting parameters that could reliably be characterized by the least-squares analysis. We found in general that globally fitting two or more spectra from different tilt angles removes a significant amount of correlation among the fitting parameters in comparison to fits carried out for disordered samples or even for a single tilt angle. Thus, the use of aligned samples in conjunction with global multicomponent least-squares analysis generally increases the number of parameters that can be independently determined, and significantly enhances the resolution to dynamic parameters of the individual components. The uncertainties in the relative amounts of each component were estimated by repeating the simulations with different starting values of the nonlinear parameters.

The magnetic tensor parameters used in the spectral calculations were: for 16-PC, $g_{xx} = 2.0089$, $g_{yy} = 2.0058$, $g_{zz} = 2.0021$, and $A_{xx} = A_{yy} = 4.9$ G $A_{zz} = 33.0$ G; for CSL $g_{xx} = 2.0089$, $g_{yy} = 2.0058$, $g_{zz} = 2.0021$, and $A_{xx} = A_{yy} = 5.0$ G, $A_{zz} = 33.8$ G (Tanaka and Freed, 1984). The dynamic variables used in the fitting procedure included the mean rotational diffusion constant, $R = \sqrt[3]{R_\perp^2 R_\parallel}$, and the rotational anisotropy parameter $N = R_\parallel/R_\perp$, where $\parallel$ and $\perp$ refer to the z axis in the principal rotational diffusion frame, i.e., the long axis of the spin labeled molecule.

The orientational distribution of the spin labeled molecules is determined by a potential which may be expanded in a series of Wigner rotation matrix elements $D^L_{0K}(\Omega)$ as follows:

$$-\frac{U(\Omega)}{kT} = \sum_{LK} \epsilon^L_K D_{0K^L}(\Omega) \tag{1}$$

where k is Boltzmann's constant and $\Omega \equiv (\alpha, \beta, \gamma)$ represents the Euler angles specifying the orientation of the molecular diffusion axes with respect to the main ordering axis of the membrane. Only the coefficients ϵ^2_0 and ϵ^2_2 were utilized in the fitting procedure. The order parameter S is defined as

$$S \equiv \langle D^2_{00} \rangle = \langle \tfrac{1}{2}(3\cos^2\theta - 1) \rangle = \frac{\int d\Omega \exp(-U(\Omega)/kT) D^2_{00}(\Omega)}{\int d\Omega \exp(-U(\Omega)/kT)}. \tag{2}$$

RESULTS

16-PC in aligned DPPC membranes

Fig. 2 shows a temperature study of the 16-PC spin probe in DPPC vesicles aligned by ISDU and hydrated to 20 wt % H_2O. ESR spectra were measured over an extensive temperature range including the gel and liquid crystalline phases for two orientations of the normal to the membrane plane with respect to the magnetic field, (i.e., for director tilt angles $\Psi = 0°$ and $\Psi = 90°$). The least-squares spectral simulations are plotted as dotted lines in Fig. 2, and the corresponding least-squares parameters given in Table 1. As shown in the table, $R_\perp$ and the order parameters could be obtained with

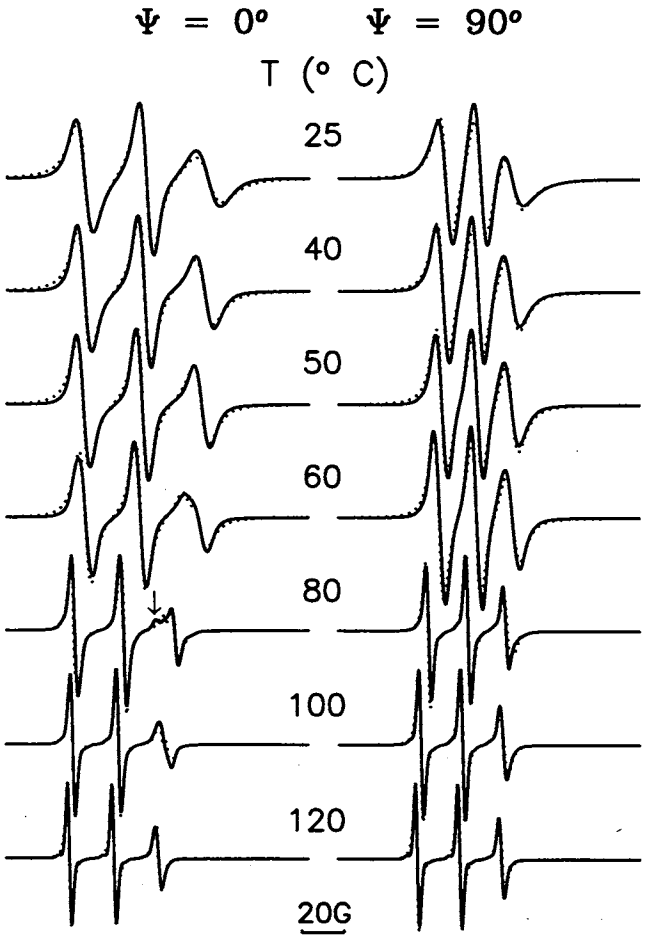

FIGURE 2 ESR spectra of the 16-PC spin probe (0.5 mol %) in DPPC membranes aligned by ISDU and hydrated to 20 wt % water over a range of temperatures in the gel and liquid crystalline phases. Spectra were measured with the field direction parallel ($\Psi = 0°$) and perpendicular ($\Psi = 90°$) to the membrane normal. (——) experimental spectra; (····) simulations. Parameters obtained from the simulations are listed in Table 1. An arrow indicates a minor component.

high accuracy. We found that the simulations were quite insensitive to the ratio $R_\parallel/R_\perp$ for 16-PC, consistent with previous studies (Kar et al., 1985; Shin and Freed, 1989a).

Below the gel to liquid crystalline transition temperature, 50°C, the spectra exhibit the simple three-line spectrum characteristic of a single component for both orientations, but with a large difference in the apparent line splittings in the spectra for $\Psi = 0°$ and $\Psi = 90°$. These results clearly indicate a single, well-ordered component in the membranes at physiologically relevant temperatures (e.g., $S \approx 0.27$ at 40°C, cf. Table 1). As the temperature is increased, the difference in the apparent splittings at the two orientations decreases and the lines narrow appreciably, reflecting lower ordering and faster motions at the higher temperatures (cf. Table 1).

In the liquid crystalline phase, an additional component (e.g., 23% at 80°C) appears, which is most discernible as a secondary high-field peak in the spectra for $\Psi = 0°$ (marked by an arrow in Fig. 2, 80°C). This component reflects a second population of spin probes with a nearly isotropic ordering and somewhat higher rotational mobility (cf. Table 1). The two peaks are distinct at intermediate temperatures (in the range of 65–95°C) but gradually merge as the temperature is increased. Above 120°C only a single three-line spectral component is observed with a slightly greater apparent splitting for $\Psi = 0°$ than that for $\Psi = 90°$, indicating that the membrane is still well aligned, although the ordering is low ($S \approx 0.03$, cf. Table 1).

The spectra were reversible with temperature over the entire temperature range studied; the spectra obtained during the cooling cycle were identical to those obtained at the same temperature during the heating cycle for each sample studied. Similar behavior was observed with a range of different samples including DPPC membranes hydrated to different water contents between 10 and 25 wt %, membranes prepared with dimyristoyl phosphatidylcholine (DMPC), and membranes labeled with the 5-doxyl stearic acid spin label. In all cases, there was no evidence of misalignment as monitored by microscopic polarimetry.

The order parameter of 16-PC obtained from the simulations is plotted as a function of temperature in Fig. 3. For comparison, the order parameter of 16-PC in pressure-annealed samples with 7 wt % water (Tanaka and Freed, 1985) is also shown.

CSL in aligned DPPC membranes

The CSL spin probe differs from 16-PC in that it exhibits substantially higher ordering and slower, much more anisotropic motion. Also, because the molecular ordering axis of CSL corresponds most closely with the magnetic y axis (i.e., CSL is "y-ordered"), the narrowest splitting appears for the $\Psi = 0°$ orientation, whereas the narrowest splitting for the z-ordered 16-PC spin probe appears for $\Psi = 90°$. Fig. 4 shows ESR spectra from CSL-labeled DPPC membranes obtained over a temperature range similar to that studied using 16-PC.

CSL also differs from 16-PC in that it may undergo hydrogen bonding with water or the oxygen atoms of lipid molecules near the membrane surface. Several lines of evidence suggest that the 3β-hydroxyl group of cholesterol is hydrogen-bonded to the acyl carbonyl group of membrane lipids, including ^{13}C-NMR (Keogh et al., 1973; Forbes et al., 1988; Sankaram and Thompson, 1991), and Fourier-transform infrared (Wong et al., 1989) measurements, as well as molecular model calculations for a 1:1 DMPC/cholesterol complex, which exhibit an energy minimum for the hydrogen-bonded structure (Vanderkooi, 1994). In principle, the 3-doxyl spin label group of CSL may engage in analogous hydrogen bonding interactions. It has been found that CSL closely resembles cholesterol in its "condensing effect" on lipid membranes (Cadenhead and Muller-Landau, 1977; De Kruijff et al., 1972). Finally, Kar et al. (1985) have reported ESR evidence for hydrogen bonding of the doxyl group of CSL. At temperatures below 0°C in pressure-annealed DPPC membranes (4–7 wt % water), they observed CSL spectra that exhibited two distinct spin probe popula-

TABLE 1 Parameters obtained from nonlinear least-squares fitting of ESR spectra of 16-PC in ISDU-aligned DPPC bilayers

T(°C)	Ph	C	$R_\perp$ (s^{-1})	ϵ_0^2	ϵ_2^2	S	P
25	G		$(9.33 \pm 0.21) \times 10^7$	1.59 ± 0.02	-1.15 ± 0.04	0.28	
40	G		$(1.99 \pm 0.03) \times 10^8$	2.48 ± 0.01	-2.66 ± 0.01	0.27	
50	G		$(2.79 \pm 0.05) \times 10^8$	2.13 ± 0.01	-2.19 ± 0.01	0.27	
60	L	1	$(2.70 \pm 0.05) \times 10^8$	1.44 ± 0.01	-1.02 ± 0.03	0.27	0.70
		2	$(3.38 \pm 0.12) \times 10^8$	0.52 ± 0.01	-0.16 ± 0.02	0.11	0.30
						($\bar{S} = 0.22$)	
80	L	1	$(3.74 \pm 0.13) \times 10^8$	0.62 ± 0.01	-0.05 ± 0.02	0.13	0.77
		2	$(2.99 \pm 0.20) \times 10^8$	0.04 ± 0.03	0.41 ± 0.05	0.00	0.23
						($\bar{S} = 0.13$)	
100	L	1	$(4.13 \pm 0.15) \times 10^8$	0.43 ± 0.01	-0.09 ± 0.01	0.09	0.57
		2	$(5.86 \pm 0.17) \times 10^8$	0.07 ± 0.01	0.23 ± 0.01	0.01	0.43
						($\bar{S} = 0.06$)	
120	L		$(5.67 \pm 0.09) \times 10^8$	0.13 ± 0.00	-0.14 ± 0.01	0.03	

T, temperature; C, component; Ph, phase; G, gel phase; L, liquid crystalline phase; P, population; $\bar{S}$, average order parameter, defined as $\Sigma_i S_i P_i$, where S_i and P_i are the order parameter and population of the ith component, respectively. A tensor components used in the simulations: $A_{xx} = A_{yy} = 4.9$ G, $A_{zz} = 33.0$ G. For 16-PC, the spectral lineshapes are sensitive to $R_\perp$ but are insensitive to the anisotropy ratio $N \equiv R_\parallel/R_\perp$. (Kar et al., 1985; Shin and Freed, 1989a). The average error of S estimated from the errors in ϵ_0^2 and ϵ_2^2 (cf. Eq. 2) is ± 0.005. The error in P is estimated at ± 0.02 (cf. text). An error of 0.00 means that the value of the error is <0.01.

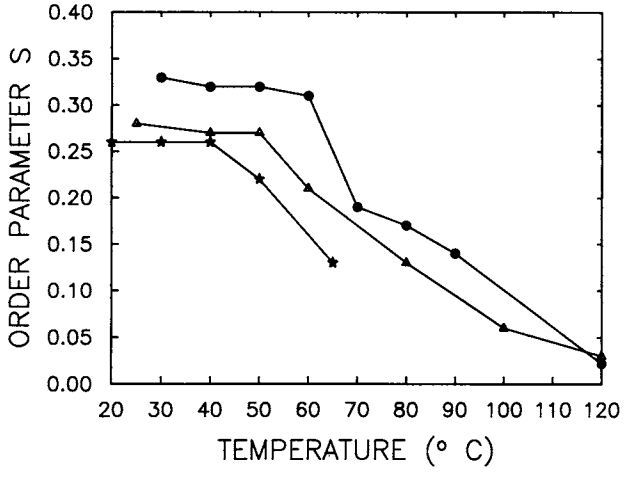

FIGURE 3 Plot of order parameter, S, of 16-PC in various aligned DPPC membranes vs. temperature. (●) Order parameters of 16-PC in DPPC membranes containing 7 wt % water aligned by pressure-annealing method (Tanaka and Freed, 1984); (△) average order parameter of 16-PC in ISDU-aligned DPPC membranes containing 20 wt % water (cf. Table 1); (★) average order parameter of 16-PC in ISDU-aligned DPPC membranes containing 0.24 mol % BR and hydrated under the same conditions that yield 20 wt % water in BR-free samples.

tions with different hyperfine tensors, which they attributed to hydrogen-bonded and non-hydrogen-bonded spin probes. Similar two-component CSL spectra were observed in the present work for ISDU-aligned DPPC membranes at very low temperature (−120°C), as is evident from the clearly resolved pairs of outer peaks in the 0° spectrum and prominent outer shoulders in the 90° degree spectrum marked by the arrows in Fig. 4. When we compare the molecular structure of CSL with cholesterol, we can see that in CSL the —NO moiety is linked to the 3-C atom and located in the β face of the molecule, i.e., —NO is a 3-β moiety, like the 3-β moiety in cholesterol. Thus the —NO moiety is also suitable for hydrogen bonding with the acyl carboxyl group (Demel et al., 1972).

Based on these considerations, we utilized a two-site model in our least-squares analysis of the CSL spectra. We first determined the magnetic parameters for each of the two "sites" by fitting the low-temperature spectra (−120°C) using rotational diffusion rates slow enough to produce rigid limit spectra ($R = 10^5\ s^{-1}$). Since differences in g values due to hydrogen bonding are expected to be unresolvable at conventional ESR frequencies (Earle et al., 1994), the same g values were used for both sites. The two values of A_{zz} could be determined from the rigid limit spectra with good accuracy, and were found to be 36.5 G and 33.8 G. The component with higher A_{zz} reflects a more polar environment (Griffith el al., 1974), and we identify it with a hydrogen-bonded CSL species. The values of A_{xx} and A_{yy} for both species could not be determined independently from the orientational order parameters in the rigid limit. We therefore set $A_{xx} = A_{yy} = 5.0$ G for the species with $A_{zz} = 33.8$ G (Kar et al., 1985; Tanaka and Freed, 1984; Meirovitch and Freed, 1984), and scaled the other A_{xx} and A_{yy} values according to the ratio of the A_{zz} components.

The hydrogen-bonded component exhibited a rather large inhomogeneous line width, which likely reflects a distribution of hyperfine values in the sample due to different hydrogen bond lengths. Although this effect is only approximately represented by adding Gaussian line broadening to the spectra, the rigid limit line shape was still reasonably well reproduced by the simulation (cf. top spectra in Fig. 4).

The least-squares simulations for the slow-motional spectra of CSL parameters based on the rigid limit magnetic parameters are shown by the dotted lines in Fig. 4, and the dynamic parameters obtained from this analysis are reported in Table 2. The two-site hydrogen bonding model was used throughout the gel phase, since it provided significantly better fits than have been obtained previously for CSL in aligned membranes utilizing only one component (cf. Kar et al., 1985; Tanaka and Freed, 1984). Fig. 5 compares one-component and two-component fits for the 30°C gel phase spectrum. The one-site simulation (dotted line in Fig. 5 *A*) qualitatively resembles previous simulations of CSL gel phase spectra (Kar et al., 1985; Tanaka and Freed, 1984), but

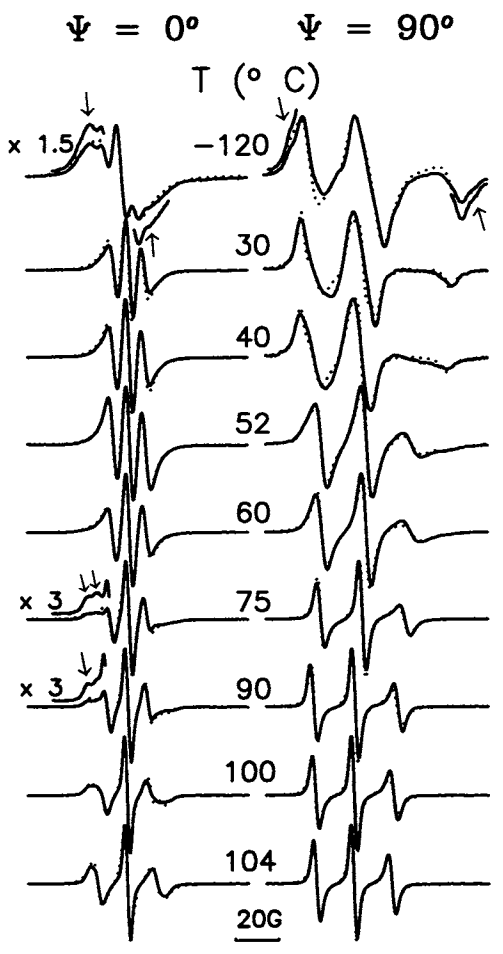

FIGURE 4 ESR spectra of the CSL spin probe (0.5 mol %) in DPPC membranes aligned by ISDU and hydrated to 20 wt % water over a range of temperatures in the gel and liquid crystalline phases. The spectra shown for −120°C correspond to the rigid limit. Spectra were measured with the field direction parallel ($\Psi = 0°$) and perpendicular ($\Psi = 90°$) to the membrane normal. (——) experimental; (····) simulations. At −120°C, both $\Psi = 0°$ and 90° spectra show two components; the second component is indicated by arrows. The −120°C, rigid limit spectra, were simulated first, from which the A tensor components of both hydrogen- and non-hydrogen-bonded species of CSL were obtained. At 75°C and 90°C arrows indicate additional components. Parameters obtained from the simulations are listed in Table 2.

it fails to reproduce the flat feature on the high-field side of the $\Psi = 90°$ spectrum. In contrast, this feature is well reproduced by a two-site model, as shown in Fig. 5 *B*, which also shows the spectra of the individual components.

In general, the nonlinear parameters for the individual sites were reasonably distinguishable in the two-site fits. Table 3 shows a correlation matrix for the least-squares parameters obtained at 30°C, which represents the degree to which the different diffusional and ordering parameters may be distinguished from one another in the least-squares solution. As can be seen from Table 3, the fitting parameters of the different sites are generally not strongly correlated, with just the exception of the $R_\parallel$ for the two species.

In the liquid crystalline phase above 75°, the spectra no longer unambiguously support the two-site hydrogen-bonding model for CSL (note the disappearance of the flat region and emergence of a peak on the high-field side of the $\Psi = 90°$ spectrum between 60°C and 90°C). This may result from rapid exchange of hydrogen bonds at higher temperatures, or from a lack of resolution due to spectral averaging by the faster molecular motions. Thus, a single, average set of hyperfine tensor parameters was used in the fits above 75°, with $A_{xx} = A_{yy} = 5.2$ and $A_{zz} = 35.2$.

However, spectra in the liquid crystalline phase do clearly reflect a second component of a different nature, specifically a component with lower ordering similar to that reported by 16-PC. This component is most evident from the additional set of outer peaks that are resolved in the $\Psi = 0°$ spectrum above 75°C, as indicated by the arrow in Fig. 4. The spectra obtained at 75°C appear to us to represent a transitional result between the lower temperatures which shows the two-site hydrogen-bonding and the higher temperatures that exhibit two components with sharply different ordering (cf. the arrows on the low-field side of the $\Psi = 0°$ spectrum). The best fit to the 75° spectra that we obtained was with 3 components, which includes the two-site hydrogen bonding and the low-ordered component.

Fig. 6 shows a plot of $R_\perp$ and $R_\parallel$ for each of the different CSL components versus temperature. Interestingly, the rotational diffusion rates of the hydrogen-bonded species in the gel phase are found to be much faster than those of the non-bonded species, which would imply location in a more fluid region of the bilayer. For example, at 30°C, the $R_\perp$ ($R_\parallel$) of the hydrogen-bonded species, $2.51 \times 10^6\ s^{-1}$ ($7.94 \times 10^7\ s^{-1}$) is about (over) an order of magnitude larger than that of the non-bonded CSL, $2.69 \times 10^5\ s^{-1}$ ($2.51 \times 10^6\ s^{-1}$). In contrast, the $R_\perp$ values of the two components in the liquid crystalline phase are similar.

In the low-temperature gel phase, both the hydrogen-bonded and non-hydrogen-bonded spin probes are highly ordered: for example, at 30°C, their order parameters are 0.79 and 0.73, respectively. In the liquid crystalline phase, the major component remains well ordered (e.g., $S = 0.48$ at 90°C) while a component appears with low ordering ($S = 0.08$), similar to what is observed using the 16PC probe. Upon further increase in temperature, the resolvable difference in ordering between the two components gradually decreases until the peaks merge at about 130°C (data not shown).

Fig. 7 compares the average order parameter $\bar{S}$ of CSL in the ISDU-aligned samples with that reported for CSL in the pressure-annealed samples (Tanaka and Freed, 1984). The data show a very similar temperature dependence, with the exception that the ISDU samples exhibit slightly lower ordering and a lower phase transition temperature, ~50°C vs. ~60°C for pressure-annealed samples. These differences may be attributed to the higher water content in the ISDU samples, as discussed below.

CSL in aligned DPPC membranes containing GA

Fig. 8 shows a temperature study of the CSL spin probe in DPPC membranes containing 2.0 mol % of the peptide GA together with the least-squares spectral simulations (dotted lines). The gel phase spectra exhibit very noticeable differences from those obtained with peptide-free membranes (cf.

TABLE 2 Parameters obtained from nonlinear least-squares fitting of ESR spectra of CSL in ISDU-aligned DPPC bilayers

T(°C)	Ph	C	$R_\perp$ (s^{-1})	$R_\parallel$ (s^{-1})	ϵ_0^2	S	P
30	G	1	$(2.51 \pm 0.11) \times 10^6$	$(7.94 \pm 1.33) \times 10^7$	5.31 ± 0.06	0.79	0.61
		2	$(2.69 \pm 0.24) \times 10^5$	$(2.51 \pm 0.32) \times 10^6$	4.21 ± 0.03	0.73	0.39
						($\bar{S}$ = 0.77)	
40	G	1	$(3.55 \pm 1.73) \times 10^6$	$(8.71 \pm 5.00) \times 10^7$	4.76 ± 0.22	0.76	0.65
		2	$(2.09 \pm 0.94) \times 10^5$	$(7.76 \pm 4.04) \times 10^6$	3.71 ± 0.10	0.68	0.35
						($\bar{S}$ = 0.73)	
52	G	1	$(5.01 \pm 0.00) \times 10^6$	$(2.00 \pm 1.15) \times 10^8$	4.58 ± 0.12	0.75	0.59
		2	$(2.77 \pm 0.18) \times 10^5$	$(2.56 \pm 0.32) \times 10^7$	3.39 ± 0.09	0.65	0.41
						($\bar{S}$ = 0.73)	
60	L	1	$(7.08 \pm 2.40) \times 10^6$	$(2.09 \pm 0.51) \times 10^8$	4.08 ± 0.07	0.72	0.53
		2	$(9.33 \pm 2.72) \times 10^5$	$(1.05 \pm 0.26) \times 10^8$	2.85 ± 0.05	0.58	0.47
						($\bar{S}$ = 0.65)	
		1	$(1.00 \pm 0.00) \times 10^7$	$(2.94 \pm 0.36) \times 10^8$	3.26 ± 0.04	0.63	0.53
75	L	2	$(2.26 \pm 0.00) \times 10^7$	$(8.07 \pm 1.15) \times 10^8$	1.59 ± 0.04	0.35	0.26
		3	$(2.19 \pm 0.14) \times 10^7$	$(6.19 \pm 0.73) \times 10^8$	0.29 ± 0.00	0.06	0.21
						($\bar{S}$ = 0.44)	
90	L	1	$(2.24 \pm 0.00) \times 10^7$	$(5.89 \pm 0.64) \times 10^8$	2.26 ± 0.04	0.48	0.73
		2	$(1.93 \pm 0.02) \times 10^7$	$(1.07 \pm 0.12) \times 10^9$	0.41 ± 0.01	0.08	0.27
						($\bar{S}$ = 0.37)	
100	L	1	$(3.47 \pm 0.00) \times 10^7$	$(5.75 \pm 0.38) \times 10^8$	1.15 ± 0.02	0.33	0.61
		2	$(3.16 \pm 0.07) \times 10^7$	$(1.12 \pm 0.41) \times 10^9$	0.27 ± 0.02	0.06	0.39
						($\bar{S}$ = 0.22)	
104	L		$(2.98 \pm 0.09) \times 10^7$	$(2.40 \pm 0.26) \times 10^9$	0.91 ± 0.01	0.20	

T, temperature; C, component; Ph, phase; G, gel phase; L, liquid crystalline phase; P, population; $\bar{S}$, average order parameter, defined as $\Sigma_i S_i P_i$, where S_i and P_i are the order parameter and population of the ith component, respectively. The A tensor components used in the simulations for the ESR spectra listed above were obtained from simulation of the rigid limit spectrum obtained at −120°C (see text). The values of these A tensor components: at and below 75°C, $A_{xx} = A_{yy} = 5.4$ G, $A_{zz} = 36.5$ G for component 1 and $A_{xx} = A_{yy} = 5.0$ G, $A_{zz} = 33.8$ G for components 2 and 3; and above 75°C, $A_{xx} = A_{yy} = 5.2$ G, $A_{zz} = 35.2$ G for all components. The average error of S estimated from errors in ϵ_0^2 and ϵ_2^2 (cf. Eq. 2) is ±0.005. The error in P is estimated at ±0.02 (cf. text). An error of 0.00 means that the value of the error is <0.01. ϵ_2^2 is typically small for CSL (Shin and Freed, 1989a; Ge et al., 1994). We fixed it at typical small values to reduce the otherwise extensive number of parameters to fit (cf. Table 3).

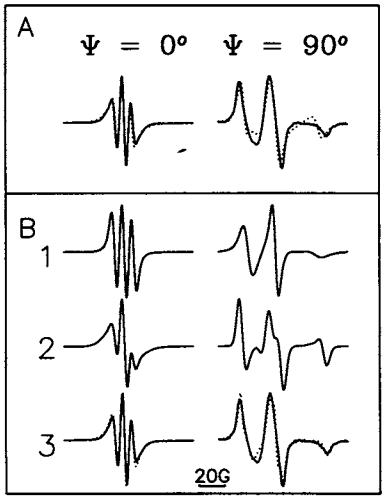

FIGURE 5 Best one- and two-component fits to the ESR spectra of CSL spin probe in DPPC membranes at 30°C from Fig. 4. (*A*) Experimental (——) and best single component fit (····) based on nonlinear least squares; (*B*) 1 and 2 correspond to the predicted spectra from the two components described by parameters listed in Table 2; 3, the composite spectra (····) compared with the experimental spectra (——).

Fig. 4), i.e., the appearance of an additional spectral component with broad features, which was previously observed by Tanaka and Freed (1985) from pressure-annealed DPPC/GA samples at low water content. This broad component could not be fit within the context of the two-site hydrogen bonding model used in the absence of GA, since an unreasonable increase in the A tensor components of one of the species would be required. Of course, a physically sounder model must take into account the inhomogeneity in the ordering of the lipid bilayers that results from incorporation of the GA (Tanaka and Freed, 1985; Williams et al., 1990). In this spirit, we retained the two components found in the absence of GA, and introduced a third, low-ordered component corresponding to the broad spectral wings associated with GA. In fact, a reasonable, but not quite as good, fit could be obtained at the lowest temperature (25°C) using only two components corresponding to ordered and disordered spin probes (results not shown). Although there was no clear statistical criterion for preferring the three-site model in this case, despite its lower χ^2, we do note that it predicts ordering and relative mobilities for hydrogen-bonded vs. non-hydrogen-bonded species similar to those found in the absence of GA (cf. Tables 2 and 4).

At temperatures above 25°C in the gel phase, there is clear evidence for the presence of three components with different ordering properties, which appear as two sets of resolved peaks outside the three central peaks of the $\Psi = 0°$ spectrum, marked "a" and "b" in Fig. 8. The A tensors for these components were taken to be the same as that of non-hydrogen-bonded CSL. As the temperature is raised, the population of the low-ordered component (reflected by the intensity of peak *a* in Fig. 8) decreases and that of a more ordered component (reflected by the intensity of peak *b*) increases over this temperature range.

In the liquid crystalline phase, the broad low-ordered component disappears, as was also observed by Tanaka and Freed (1985). The gel to liquid crystal transition temperature in

TABLE 3 Correlation matrix for the parameters obtained from nonlinear least-squares fitting of ESR spectra of CSL in the ISDU-aligned DPPC membrane at 30°C

	T_{20}^{-1}	$R_\perp(1)$	$R_\perp(2)$	$R_\parallel(1)$	$R_\parallel(2)$	$\epsilon_0^2(1)$	$\epsilon_0^2(2)$
T_{20}^{-1}	1.0000	−.5110	.2487	−.2139	.2090	−.1763	.0258
$R_\perp(1)$		1.0000	−.2710	−.3414	.3371	−.2392	.3066
$R_\perp(2)$			1.0000	−.6074	.6145	−.6803	.1812
$R_\parallel(1)$				1.0000	−.9859	.6040	−.1465
$R_\parallel(2)$					1.0000	−.6407	.1672
$\epsilon_0^2(1)$						1.0000	−.7890
$\epsilon_0^2(2)$							1.0000

An element in the correlation matrix, r_{ab}, the so called correlation coefficient, is defined as: $r_{ab} = \langle (a - \bar{a})(b - \bar{b}) \rangle / \sqrt{\langle (a - \bar{a})^2 (b - \bar{b})^2 \rangle}$. a, b are two of the parameters varied in the simulations.

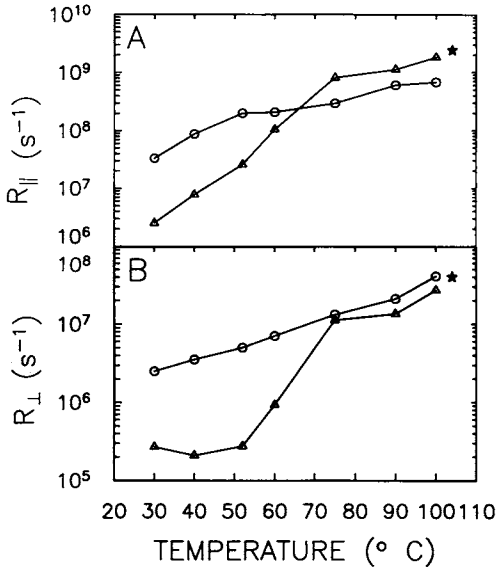

FIGURE 6 Plot of $R_\parallel$ (A) and $R_\perp$ (B) of hydrogen-bonded CSL (○) and non-hydrogen-bonded CSL (△) in ISDU-aligned DPPC membranes vs. temperature. (★) Datum from one-component simulation of the spectrum at 104°C.

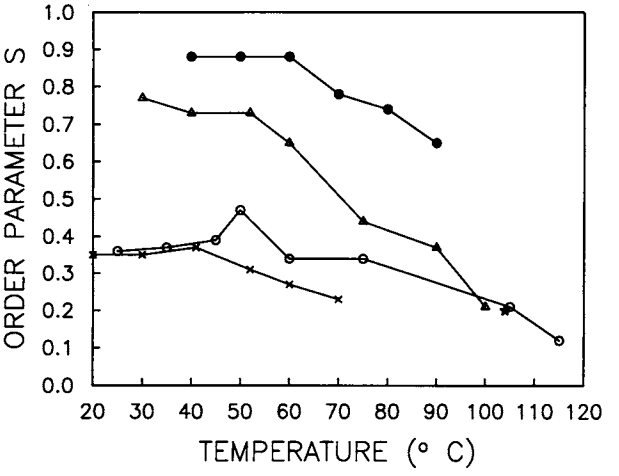

FIGURE 7 Plot of average order parameter, $\bar{S}$, of CSL in various aligned DPPC membranes vs. temperature. (●) Average order parameter of CSL in DPPC membranes containing 7 wt % water aligned by pressure-annealing method (Tanaka and Freed, 1984); (△) average order parameter of CSL in ISDU-aligned DPPC membranes containing 20 wt % water (cf. Table 2); (○) average order parameter of CSL in ISDU-aligned DPPC membranes containing 2 mol % GA, and hydrated under the same conditions that yield 20 wt % water in GA-free samples; (×) average order parameters of CSL in ISDU-aligned DPPC membranes containing 0.24 mol % BR and hydrated under the same conditions that yield 20 wt % water in BR-free samples; (★) datum from one-component simulation of the spectrum at 104°C.

their case was between 60° and ~ 70°C (for 2.0 mol % GA and 7 wt % water content), whereas the transition temperature we observed is between 50° and 60°C. This difference is most likely due to the difference of water content between the two samples. Above 60°C, all the spectra can be well-simulated with just a single component, implying that in the liquid crystalline phase, differences between the species are no longer resolvable on the ESR time scale. This is in contrast to the GA-free DPPC samples in which there was a clearly resolvable low-ordered second component.

The parameters obtained from the simulations are listed in Table 4, and the change in average order parameter $\bar{S}$ of CSL with temperature is plotted in Fig. 7. Significantly, a small steady *increase* in $\bar{S}$ is observed when the temperature increases from 25° to 45°C. This reflects the decrease of the low-ordered component and increase in the more highly ordered component described above. The relatively large increase in $\bar{S}$ at 50°C (from 0.39 to 0.47) results from the disappearance of these additional species, and the multicomponent spectrum is replaced by a simple single-component spectrum. The sharp decrease in $\bar{S}$ by 0.13 between 50° and 60°C corresponds to the gel-to-liquid-crystalline transition and is in good agreement with DSC results (cf. below). Above 60°C, $\bar{S}$ decreases slowly with further increases in temperature.

CSL in aligned DPPC membranes containing BR

Fig. 9 shows a series of ESR spectra obtained for the CSL spin label in DPPC membranes containing 0.24 mol % BR aligned by ISDU and hydrated under the same conditions that produce 20 wt % water in protein-free membranes. Least-squares spectral simulations are shown by the dotted lines in this figure. The temperature was varied from room temperature to ~70°C, corresponding to the gel phase and the lower end of the liquid crystalline phase. Higher temperatures were not studied to avoid denaturation of the BR.

The effect of BR on CSL throughout this temperature range is immediately apparent in the ESR spectra, (cf. Figs. 4 and 9). The plateau evident in the low-field wing of the spectrum is a good indication that at least two components are present throughout the temperature range studied in Fig.

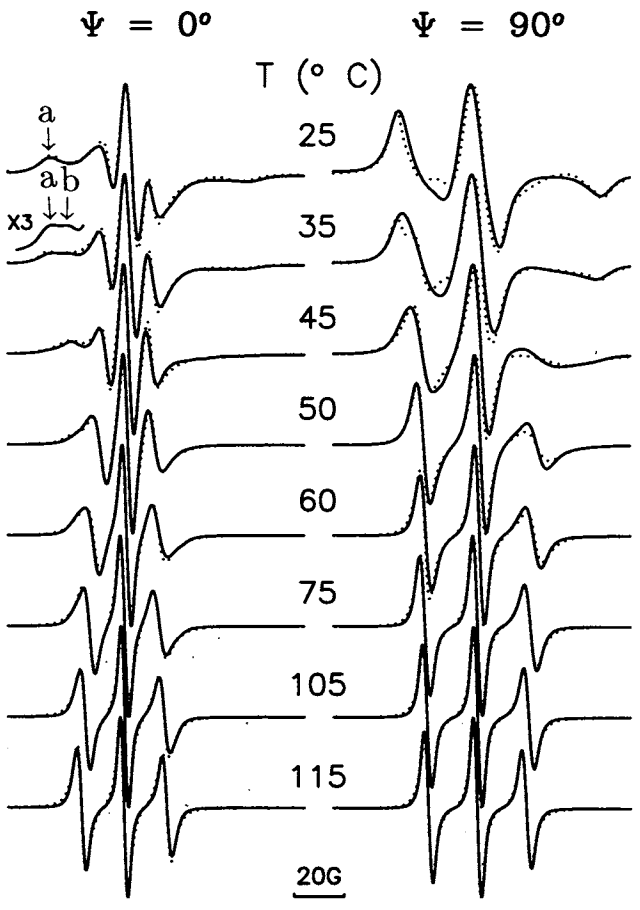

FIGURE 8 ESR spectra of the CSL spin probe (0.5 mol %) in DPPC membranes prepared with 2 mol % GA, aligned by ISDU and hydrated under the same conditions that yield 20 wt % water in GA-free samples over a range of temperatures in the gel and liquid crystalline phases. Spectra were measured with the field direction parallel (Ψ = 0°) and perpendicular (Ψ = 90°) to the membrane normal. (——) experimental spectra; (····) simulations. Parameters obtained from the simulations are listed in Table 4.

9. In fact, for the reasons described above in the analysis of the GA/DPPC system, three components were used to fit the gel phase spectra, and two were used for the liquid crystalline phase. The three components are clearly evident in the left wing of the spectrum at 41°C, with two of the peaks indicated by arrows *a* and *b*. The component *a*, corresponding to the "boundary lipids," is nearly isotropic. Parameters obtained from the least-squares fits are listed in Table 5.

The results from CSL in BR-containing membranes may be summarized as follows: 1) The ordering of the lipids in both gel and liquid crystal phases is significantly reduced by BR, which is similar to the effect of GA on the ordering of membranes. For example at 30°C (gel phase), S for the two components in the bulk lipid phase decreases from 0.79 and 0.73, respectively, to 0.51 and 0.53 upon addition of BR, and a third component with S = 0.10, corresponding to the "boundary" lipid, appears. At 60°C (liquid crystal phase), the S of the bulk phase components is reduced from 0.72, 0.58 to 0.36, while S of the "boundary" component is 0.13 (cf. Table 5). 2) The average order parameter for CSL in the BR/DPPC system exhibited a temperature dependence similar to that observed in the GA/DPPC system; i.e., $\bar{S}$ first increases between 30° and 40° and then decreases slowly with further increase in temperature, as shown in Fig. 7. 3) Just as observed in the pure DPPC and GA/DPPC systems, in the gel phase (below 52°C), the rotational diffusion rate of the hydrogen-bonded CSL probes is greater than that of the non-bonded species, but the difference is smaller than that in the pure DPPC membranes (cf. Table 5). 4) In the gel phase, the rotational mobility of the hydrogen-bonded species ($R_\perp$ and $R_\parallel$) is increased slightly by the addition of BR. For example, at 30°C the $R_\perp$ and $R_\parallel$ of component 1 increase from 2.51 × 10^6 s^{-1} and 7.94 × 10^7 s^{-1} for DPPC to 3.02 × 10^6 s^{-1} and 1.10 × 10^8 s^{-1} for BR/DPPC. In contrast, the rotational mobility of non-hydrogen-bonded CSL is increased by a factor of ~3. For example, at 30°C, the $R_\perp$ and $R_\parallel$ of component 2 increase from 2.69 × 10^5 s^{-1} and 2.51 × 10^6 s^{-1} for pure DPPC to 8.70 × 10^5 s^{-1} and 7.24 × 10^6 s^{-1} for BR/DPPC, respectively (cf. Tables 2 and 5). 5) The gel to liquid crystalline phase transition occurs at a slightly lower temperature (i.e., below 52°C) than for the GA/DPPC and pure DPPC cases. 6) In the liquid crystalline phase, there is a two-component structure that is similar to that seen in the pure DPPC case (but not the GA/DPPC case) at somewhat higher temperature. 7) No "immobilized" component due to the incorporation of BR was observed throughout the temperature range studied as was also the case for GA/DPPC systems (see Discussion).

16-PC in aligned DPPC vesicles containing BR

Fig. 10 shows an ESR temperature study of the 16-PC spin probe in ISDU-aligned DPPC membranes containing 0.24 mol % BR that was carried out under experimental conditions similar to those used in the CSL study. In contrast to the rather dramatic effects of BR observed using the CSL spin probe, the 16-PC spectra in BR-containing membranes are quite similar to those observed in BR-free membranes (cf. Figs. 2 and 10). However, the incorporation of BR into the membranes does reduce the gel to liquid crystalline transition as monitored by 16-PC (cf. Fig. 3 and Tables 1 and 6). Also, no clear evidence of a second component appears in the spectra through the temperature range studied. Parameters obtained from the simulations are given in Table 6. The simulations are plotted as dotted lines in Fig. 10. It is evident that good simulations could be obtained with just a single component for all the 16-PC spectra. As shown in Table 6 and Fig. 3, in which the order parameter of 16-PC is plotted versus temperature, the ordering near the end of the acyl chain is reduced only slightly after BR is incorporated into the membranes, e.g., from 0.27 to 0.26 at 40°C. $R_\perp$ is also reduced by incorporation of BR, e.g., $R_\perp$ decreases from 1.99 × 10^8 to 1.45 × 10^8 s^{-1} at 40°C (cf. Tables 1 and 6).

DSC

Fig. 11 shows the DSC traces for ISDU-aligned DPPC membranes containing 20 wt % H_2O with no added protein or peptide, and Figs. 12 and 13 show DSC traces for those

TABLE 4 Parameters obtained from nonlinear least-squares fitting of ESR spectra of CSL in DPPC containing 2.0 mol % GA

T(°C)	Ph	C	$R_\perp$ (s^{-1})	$R_\parallel$ (s^{-1})	ϵ_0^2	S	P
25	G	1	$(5.62 \pm 3.05) \times 10^6$	$(1.08 \pm 0.74) \times 10^8$	4.46 ± 0.26	0.74	0.19
		2	$(1.26 \pm 0.54) \times 10^6$	$(4.68 \pm 1.93) \times 10^6$	3.14 ± 0.09	0.62	0.28
		3	$(1.66 \pm 0.83) \times 10^7$	$(1.26 \pm 0.66) \times 10^7$	0.09 ± 0.00	0.02	0.53
						($\bar{S} = 0.36$)	
35	G	1	$(6.31 \pm 0.00) \times 10^6$	$(1.12 \pm 0.23) \times 10^8$	4.23 ± 0.05	0.73	0.42
		2	$(2.88 \pm 0.00) \times 10^6$	$(6.61 \pm 1.71) \times 10^7$	1.28 ± 0.01	0.28	0.21
		3	$(1.63 \pm 0.07) \times 10^7$	$(4.36 \pm 0.54) \times 10^7$	0.10 ± 0.00	0.02	0.37
						($\bar{S} = 0.37$)	
45	G	1	$(1.15 \pm 0.00) \times 10^7$	$(1.26 \pm 0.14) \times 10^8$	4.72 ± 0.06	0.76	0.30
		2	$(5.01 \pm 0.00) \times 10^6$	$(9.55 \pm 1.79) \times 10^7$	1.29 ± 0.04	0.29	0.57
		3	$(1.19 \pm 0.09) \times 10^7$	$(6.17 \pm 1.50) \times 10^7$	0.05 ± 0.00	0.01	0.13
						($\bar{S} = 0.39$)	
50	G	1	$(1.55 \pm 0.64) \times 10^7$	$(1.82 \pm 0.86) \times 10^8$	2.16 ± 0.08	0.47	0.83
		2	$(5.62 \pm 2.36) \times 10^6$	$(2.34 \pm 1.14) \times 10^8$	2.22 ± 0.08	0.48	0.17
						($\bar{S} = 0.47$)	
60	L		$(3.02 \pm 0.00) \times 10^7$	$(3.94 \pm 0.05) \times 10^8$	1.51 ± 0.01	0.34	
75	L		$(4.79 \pm 0.12) \times 10^7$	$(7.24 \pm 0.16) \times 10^8$	1.53 ± 0.01	0.34	
105	L		$(6.92 \pm 0.16) \times 10^7$	$(1.45 \pm 0.07) \times 10^9$	0.94 ± 0.01	0.21	
115	L		$(1.05 \pm 0.02) \times 10^8$	$(2.63 \pm 0.12) \times 10^9$	0.56 ± 0.01	0.12	

T, temperature; C, component; Ph, phase; G, gel phase; L, liquid crystalline phase; P, population; $\bar{S}$, average order parameter, defined as $\Sigma_i S_i P_i$, where S_i and P_i are the order parameter and population of the ith component, respectively. A tensor components used in the simulations: at and below 50°C, $A_{xx} = A_{yy} = 5.4$ G, $A_{zz} = 36.5$ G for component 1, and $A_{xx} = A_{yy} = 5.3$ G, $A_{zz} = 35.8$ G for components 2 and 3; at and above 60°C, $A_{xx} = A_{yy} = 5.4$ G, $A_{zz} = 36.2$ G for both components 1 and 2. The average error of S estimated from the errors in ϵ_0^2 and ϵ_2^2 (cf. Eq.2) is ± 0.005. The error in P is estimated at ± 0.02 (cf. text). An error of 0.00 means that the value of the error is <0.01. ϵ_2^2 is typically small for CSL (Shin and Freed, 1989a; Ge et al., 1994). We fixed it at typical small values to reduce the otherwise extensive number of parameters to fit (cf. Table 3).

containing 2 mol % GA and 0.24 mol % BR, respectively. In all cases, the DSC corresponds reasonably well with the behavior observed for both 16-PC and CSL by ESR. In Fig.11, two peaks appear in the DSC, one corresponding to the main (gel-to-liquid crystal) transition for DPPC, which occurs at 50°C, and a second transition at 127°C. No pretransition is observed.

The high-temperature transition is quite sharp, with a width of only 0.3°C. This transition for DPPC was first reported by Tanaka and Freed (1984) for pressure-annealed samples, but at a lower temperature (~100°C). The difference in transition temperatures may reflect the different water contents, alignment procedures and/or thermal history of the samples. There is some experimental evidence that these latter differences can modify the phase behavior of lipid membranes (Silvius and Brown, 1986).

As noted above, a minor component exhibiting low ordering in the liquid crystalline phase was observed in the ESR of 16-PC for a number of different sample preparations using different lipids, spin labels, and water contents, all of which were studied over a similar temperature range (results not shown). In all cases, the higher transition temperature measured by ESR corresponds reasonably well with that measured by DSC, although in a few cases the temperature at which the minor ESR component completely disappeared was as much as 10° lower than that measured by DSC. A possible reason for this discrepancy is that the two components with very small differences in ordering become increasingly difficult to resolve as the temperature approaches the second transition, so that the ESR peaks appear to merge at a temperature below that at which the DSC peak is observed.

In the DSC of BR-containing membranes, two peaks are apparent in the temperature range from 0° to 80°C (cf. Fig. 13). All samples exhibited a high-temperature transition at 50°C that could be identified with the main transition of the lipid phase. In addition, a broad endothermic peak was observable in all samples studied; the center of the transition ranged between 30–35°C for the different sample preparations studied. Two peaks were also observed in the DSC for both nonaligned dispersion samples (results not shown) and ISDU-aligned vesicles of DPPC incorporating 2 mol % GA (cf. Fig. 12).

DISCUSSION

Comparison of ISDU and pressure-annealing alignment

The most straightforward basis for assessing the relative degree of alignment obtainable by the ISDU and pressure-annealing methods by ESR is to compare the orientational order parameters and rotational mobilities observed for different spin probes in simple DPPC membranes aligned by each method. As noted in the Results, the gel-phase spectra of ISDU-aligned membranes consist of a single, well-ordered component for the 16-PC and two well-ordered components for CSL, corresponding to hydrogen-bonded and non-hydrogen-bonded CSL species. This interpretation is supported by the high quality of the spectral fits obtained for both spin probes in this phase, as shown in Figs. 2 and 4, that was facilitated by using the latest version of the nonlinear least-squares fitting program recently developed in this group (Budil et al., unpublished). Before a detailed comparison, we should emphasize that the "hydrogen bonding" model has allowed a significant improvement in the simulations of ESR spectra from CSL in all the ISDU-aligned lipid membrane systems studied in this work. The overall fits

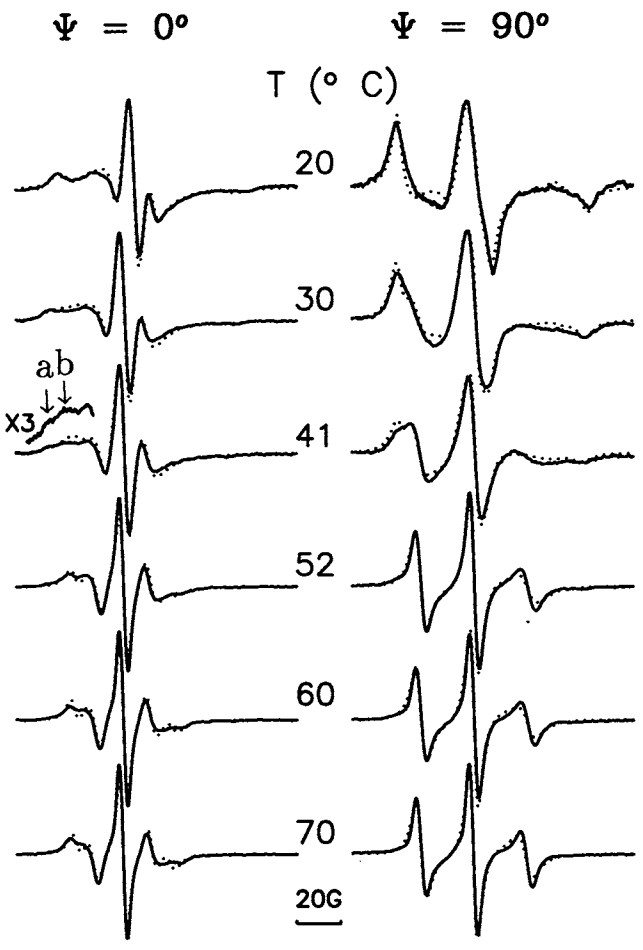

FIGURE 9 ESR spectra of the CSL spin probe (0.5 mol %) in DPPC membranes prepared with 0.24 mol % BR, aligned by ISDU, and hydrated under the same conditions that yield 20 wt % water in BR-free samples over a range of temperatures in the gel and liquid crystalline phases. Spectra were measured with the field direction parallel (Ψ = 0°) and perpendicular (Ψ = 90°) to the membrane normal. (——) experimental spectra; (····) simulations. Parameters obtained from the simulations are listed in Table 5.

are of a better quality than we have been able to achieve previously, as already noted, and they reveal a common feature in the dynamics of the spin probe CSL. That is, in the gel phase, hydrogen-bonded CSL (with larger A tensor components) undergoes faster rotational diffusion than non-hydrogen-bonded CSL probe (with smaller A tensor components). These results provide indirect evidence that the hydrogen-bonded cholesterol may reside at the interface of the lipid bilayers where they experience greater rotational mobility.

A comparison of the parameters for 16-PC summarized in Tables 1 and 7 shows that the order parameter S and the rotational diffusion rates $R_\perp$, $R_\parallel$ at 40°C are similar for ISDU-aligned and pressure-annealed samples. The larger S and smaller $R_\perp$ and $R_\parallel$ for the pressure-annealed samples are simply due to the lower water contents in the pressure-annealed samples (4–7 wt % H_2O vs. 20 wt % H_2O). For CSL, also considering the differences in the water content between the samples aligned by the different methods, the order parameters obtained for the hydrogen-bonded and non-hydrogen-bonded species, 0.76 and 0.68 at 40°C (cf. Table 2), compare favorably with the order parameters in pressure-annealed samples, 0.88 at 40°C (Tanaka and Freed, 1984). The difference in the $R_\perp$ is of the magnitude expected from differences in the water content as shown by Tanaka and Freed (1984). In general, the quality of the experimental spectra we obtain compares very favorably in appearance with those of Tanaka and Freed (1984), consistent with their good alignment.

As noted in the Results, minor additional features appear in the ESR spectra from the liquid crystalline phase for the 16-PC spin probe (and also for CSL) in the ISDU-aligned pure DPPC vesicles, indicating the presence of a minor component in the sample with significantly lower spin probe ordering. Thus, a question is raised as to the nature of such a component in the spectra of both the 16-PC and CSL spin probes. One possibility is that the difference in ordering of the second component occurs at the molecular level, so that it corresponds to a second phase with lower molecular ordering. We note that two-phase spectra similar to those shown in Figs. 2 and 4 have been observed in the liquid crystal phases of DPPC for both 16-PC and CSL in pressure-annealed membranes when the temperature is poised at the phase transition between liquid crystalline and high temperature phases (Tanaka and Freed, 1984). A second possibility is that disorder is occurring on a macroscopic level; i.e., the molecular ordering of the spin probe remains relatively high in local membrane domains, but the local directors of individual membrane fragments are themselves disordered, i.e., the MOMD effect (Meirovitch et al., 1984). This type of disorder could reflect defects or artifacts from the ISDU alignment procedure that result in incomplete alignment of the membranes.

There are several lines of evidence which strongly suggest that the minor component in the spectra from 16-PC does not arise from artifacts in the alignment procedure. As noted in the Results, the coexisting components appear reproducibly in the liquid crystal phase only, and there was no indication of any macroscopic membrane misalignment by room-temperature microscopic polarimetry in any of the samples studied by ESR. Also, the appearance and disappearance of the additional structure in the liquid crystal phase ESR spectra is completely reversible with temperature, suggesting that it is related to the temperature-dependent phase behavior of the membrane rather than just a static macroscopic misalignment. For the gel phase of the lipid, the observation of just a single component with excellent ordering for 16-PC and the observation of a well-ordered CSL spectrum (i.e., both hydrogen-bonded and non-hydrogen-bonded components are well ordered), provides strong indication that the membranes are macroscopically well aligned. Any defects exhibiting MOMD-like disorder would appear as a set of outer peaks at the lower temperatures (most prominently for 0° director tilt in the CSL spectra and for 90° in the 16-PC spectra), which are not observed. Finally, there was no hint of any misaligned component in the liquid crystalline phase in any of the GA-containing samples studied (cf. Fig. 8),

TABLE 5 Parameters obtained from nonlinear least-squares fitting of ESR spectra of CSL in DPPC containing 0.24 mol % BR

T(°C)	Ph	C	$R_\perp$ (s^{-1})	$R_\parallel$ (s^{-1})	ϵ_0^2	S	P
20	G	1	$(2.63 \pm 0.02) \times 10^6$	$(4.25 \pm 0.55) \times 10^7$	3.09 ± 0.03	0.61	0.22
		2	$(1.05 \pm 0.09) \times 10^6$	$(3.80 \pm 0.25) \times 10^6$	2.24 ± 0.01	0.48	0.37
		3	$(1.02 \pm 0.09) \times 10^7$	$(1.58 \pm 0.25) \times 10^7$	0.49 ± 0.00	0.10	0.41
						($\bar{S}$ = 0.35)	
30	G	1	$(3.02 \pm 0.62) \times 10^6$	$(1.10 \pm 0.38) \times 10^8$	2.45 ± 0.05	0.51	0.25
		2	$(8.70 \pm 0.89) \times 10^5$	$(7.24 \pm 0.79) \times 10^6$	2.55 ± 0.04	0.53	0.35
		3	$(1.45 \pm 0.41) \times 10^7$	$(3.55 \pm 0.99) \times 10^7$	0.46 ± 0.00	0.10	0.40
						($\bar{S}$ = 0.35)	
40	G	1	$(3.72 \pm 0.74) \times 10^6$	$(1.32 \pm 0.24) \times 10^8$	2.06 ± 0.02	0.44	0.47
		2	$(1.86 \pm 0.21) \times 10^6$	$(1.41 \pm 0.29) \times 10^7$	2.17 ± 0.03	0.47	0.28
		3	$(1.66 \pm 0.25) \times 10^7$	$(4.17 \pm 0.24) \times 10^7$	0.51 ± 0.00	0.11	0.25
						($\bar{S}$ = 0.37)	
52	L	1	$(1.29 \pm 0.01) \times 10^7$	$(1.86 \pm 0.19) \times 10^8$	1.86 ± 0.01	0.40	0.64
		2	$(5.01 \pm 0.07) \times 10^6$	$(4.27 \pm 0.08) \times 10^8$	0.64 ± 0.00	0.14	0.36
						($\bar{S}$ = 0.31)	
60	L	1	$(2.24 \pm 0.00) \times 10^7$	$(1.78 \pm 0.08) \times 10^8$	1.67 ± 0.01	0.36	0.61
		2	$(1.10 \pm 0.03) \times 10^7$	$(9.55 \pm 0.42) \times 10^8$	0.62 ± 0.01	0.13	0.39
						($\bar{S}$ = 0.27)	
70	L	1	$(2.99 \pm 1.07) \times 10^7$	$(1.74 \pm 1.40) \times 10^8$	1.58 ± 0.05	0.34	0.54
		2	$(2.00 \pm 0.66) \times 10^7$	$(1.38 \pm 0.31) \times 10^9$	0.49 ± 0.01	0.10	0.46
						($\bar{S}$ = 0.23)	

T, temperature; C, component; Ph, phase; G, gel phase; L, liquid crystalline phase; P, population; $\bar{S}$, average order parameter, defined as $\Sigma_i S_i P_i$, where S_i and P_i are the order parameter and population of the ith component, respectively. The average error of S estimated from the errors in ϵ_0^2 and ϵ_2^2 (cf. Eq. 2) is ±0.005. The error in P is estimated at ±0.02 (cf. text). An error of 0.00 means that the value of the error is <0.01. A tensor components used in the simulations: at and below 41°C, $A_{xx} = A_{yy}$ = 5.4 G, A_{zz} = 36.5 G for component 1; $A_{xx} = A_{yy}$ = 5.3 G, A_{zz} = 34.8 G for components 2 and 3; at and above 52°C, $A_{xx} = A_{yy}$ = 5.4 G, A_{zz} = 35.6 G for both components 1 and 2. ϵ_2^2 is typically small for CSL (Shin and Freed, 1989a; Ge et al., 1994). We fixed it at typical small values to reduce the otherwise extensive number of parameters to fit (cf. Table 3).

which would be expected if such features were due to an artifact of the membrane alignment procedure.

For the ESR spectra from CSL, two-component spectra emerge from our analysis through the whole temperature range studied except at 75°C. In the gel phase, they are from hydrogen-bonded and non-hydrogen-bonded CSL molecules. However, in the liquid crystalline phase, we cannot distinguish these two types of CSL, possibly because of spectral averaging due to the enhanced motion. We do, however, observe two components with different ordering which most likely have the same origin as those of the 16-PC spectra described above.

We conclude that the ISDU-aligned membranes are well aligned in both the gel and liquid crystalline phases and that the additional features observed in the liquid crystal region are peculiar to that phase. These additional components may arise from the presence of (metastable) coexisting phases with different temperature-dependent ordering possibly due to special features of the ISDU alignment procedure. For example, in the pressure-annealing procedure, the lipid bilayers are annealed at about 20°C above the gel-to-liquid crystal transition temperature, T_c, to achieve the fluidity needed for optimal alignment. In contrast, the ISDU sample were aligned and annealed at room temperature, i.e., below T_c. As noted above, such a difference in thermal histories of the different sample types may lead to different phase behavior in the aligned membranes. A fuller analysis of these matters was not undertaken in this work.

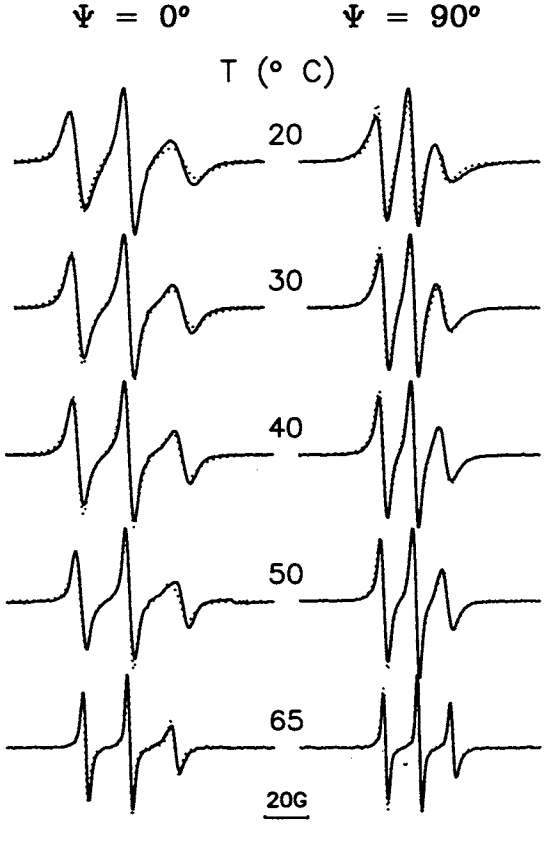

FIGURE 10 ESR spectra of the 16-PC spin probe (0.5 mol %) in DPPC membranes prepared with 0.24 mol % BR, aligned by ISDU, and hydrated under the same conditions that yield 20 wt % water in BR-free vesicles over a range of temperatures in the gel and liquid crystalline phases. Spectra were measured with the field direction parallel (Ψ = 0°) and perpendicular (Ψ = 90°) to the membrane normal. (——) experimental spectra; (····) simulations. Parameters obtained from the simulations are listed in Table 6.

Effects of GA

GA has frequently been used as a model for studying protein/lipid interactions in model membranes by the ESR spin-

TABLE 6 Parameters obtained from nonlinear least-squares fitting of ESR spectra of 16-PC in DPPC containing 0.24 mol % BR

T(°C)	Ph	$R_\perp$ (s^{-1})	ϵ_0^2	ϵ_2^2	S
20	G	$(8.71 \pm 0.20) \times 10^7$	1.47 ± 0.02	-1.10 ± 0.04	0.26
30	G	$(1.10 \pm 0.03) \times 10^8$	1.42 ± 0.04	-0.96 ± 0.03	0.26
40	G	$(1.45 \pm 0.04) \times 10^8$	1.38 ± 0.03	-0.97 ± 0.03	0.26
50	L	$(1.93 \pm 0.04) \times 10^8$	1.13 ± 0.01	-0.64 ± 0.03	0.23
65	L	$(3.24 \pm 1.29) \times 10^8$	0.64 ± 0.04	-0.23 ± 0.01	0.14

T, temperature; C, component; Ph, phase; G, gel phase; L, liquid crystalline phase; P, population; $\bar{S}$, average order parameter, defined as $\Sigma_i S_i P_i$, where S_i and P_i are the order parameter and population of the ith component, respectively. A tensor components used in the simulations: $A_{xx} = A_{yy} = 4.9$ G, $A_{zz} = 33.0$ G. For 16-PC, the spectral lineshapes are sensitive to $R_\perp$ but are insensitive to the anisotropy ratio $N \equiv R_\parallel/R_\perp$. (Kar et al., 1985; Shin and Freed, 1989a). The average error of S estimated from the errors in ϵ_0^2 and ϵ_2^2 (cf. Eq. 2) is ±0.005. The error in P is estimated at ±0.02 (cf. text). An error of 0.00 means that the value of the error is <0.01.

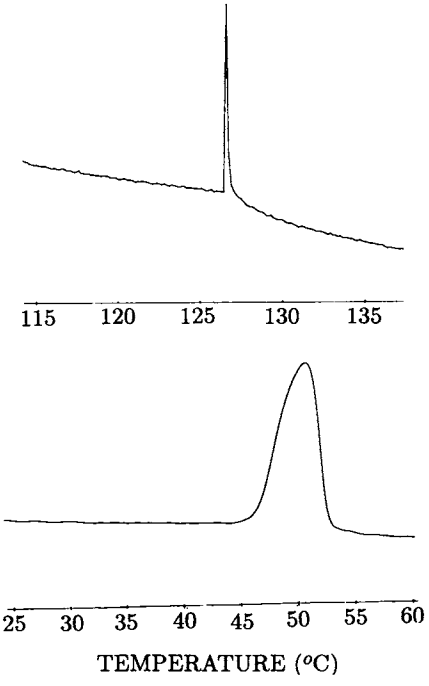

FIGURE 11 DSC scans of ISDU-aligned DPPC membranes with 20 wt % water. Scanning rate, 3°C/min.

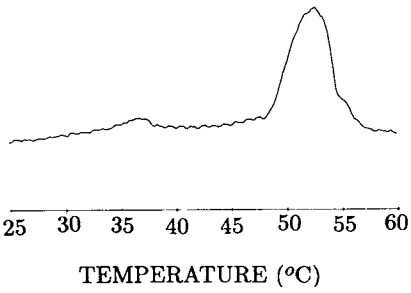

FIGURE 12 DSC scans of ISDU-aligned DPPC membranes containing 2.0 mol % GA and hydrated under the same conditions that yield 20 wt % water in GA-free samples. Scanning rate, 3°C/min.

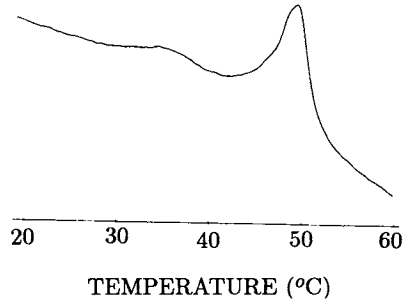

FIGURE 13 DSC scans of ISDU-aligned DPPC membranes containing 0.24 mol % BR and hydrated under the same conditions that yield 20 wt % water in BR-free samples. Scanning rate, 3°C/min.

labeling method, in part because it can withstand the rather rigorous pressure-annealing procedure needed to incorporate it into an aligned membrane. In a previous study of GA in aligned DPPC membranes (Tanaka and Freed, 1985), this peptide was found to exert two different and somewhat opposite effects on the membrane. The first was a disordering effect apparent in the gel and liquid crystal phases arising from disruption of the lipid packing by the GA, and the second was a "hardening" effect that actually increases lipid ordering in the high-temperature weakly ordered phase. In general no appreciable change in the membrane fluidity was found (Tanaka and Freed, 1985; Rice and Oldfield, 1979). Neither was any evidence found for the features usually associated with "immobilized," protein-bound lipids from the aligned samples.

The ESR spectra of CSL in the ISDU-aligned DPPC membranes containing GA are similar to those from the pressure-annealed membranes of similar composition but lower water content obtained by Tanaka and Freed (1985). The most important feature is that ESR spectra obtained in the gel phase show distinct components for the GA-containing membranes that are not observable in the GA-free samples. These components are attributable to a population of spin labels associated with the GA molecules, which exhibit significantly reduced ordering. An important difference in the two cases is that the fractional population of disordered component is much less at high water content than at low water content. Thus Tanaka and Freed (1985; Rice and Oldfield, 1979) found that 65% of the lipids were disordered by 2 mol % GA for 7 wt % water at 50°C. Our results in Table 4 for 2 mol % GA and 20 wt % water show a population of disordered lipids of 53% at 25°C, 37% at 35°C, 13% at 45°C, and too small to measure at 50°C. Within the liquid crystalline phase, only a single component is observable for both low and high water contents.

A comparison of the parameters obtained from the nonlinear least-squares fits of the ESR spectra from the ISDU-aligned samples and the earlier fits to the pressure-annealed samples exhibit a number of similar features but with differences attributable to the different water contents. They include the following: 1) In the gel phase, GA has a strong disordering effect on the lipids, which is less dramatic for high water content; e.g., at 50°C, the order parameter of CSL in a pressure-annealed DPPC sample with 7 wt % water is 0.88, but it is reduced to an average value of 0.40 after 2 mol

TABLE 7 Parameters obtained in earlier ESR studies of 16-PC and CSL in pressure-annealed DPPC bilayers

Sample	Water (wt %)	T(°C)	$R_\perp$ (s^{-1})	$R_\parallel$ (s^{-1})	ϵ_0^2	ϵ_2^2	S
16-PC							
Tanaka and Freed (1984)	7	40	1.3×10^8	2.6×10^8			0.32
Kar et al. (1985)	4	41	7.0×10^7	7.0×10^7	2.0	−1.5	0.38
CSL							
Tanaka and Freed (1984)	7	40	3.0×10^5	4.5×10^7			0.88
Kar et al. (1985)	4	22	5.0×10^5	1.3×10^7	6.0	0.0	0.82

% GA is added (Tanaka and Freed, 1985). The average order parameter of CSL in ISDU-aligned DPPC with higher water content (~ 20%) at 52°C, 0.73 is reduced to 0.47 after 2 mol % GA is added at 50°C (cf. Tables 2 and 4). 2) In the liquid crystal phase, the ordering of the lipid is reduced significantly by GA and again the effect is less pronounced for high water content. Thus at 80°C, the order parameter of CSL in the low water content DPPC sample decreases from 0.74 to 0.42 after 2 mol % GA is incorporated (Tanaka and Freed, 1985); at 75°C, addition of the same amount of GA reduces the order parameter of CSL in the high water content DPPC sample from 0.44 to 0.34. 3) At higher temperatures (above ~95°C), the GA-containing membranes actually exhibit slightly higher ordering than the GA-free membranes (cf. Fig. 7 and Tanaka and Freed, 1985). 4) In the gel phase, GA increases the rotational mobility of the lipid molecules (Lee et al., 1984). For example, at 50°C, in the low water content DPPC membranes, $R_\perp$ is $5.0 \times 10^5\ s^{-1}$, but it increases to $4.0 \times 10^6\ s^{-1}$ for the disordered component. (In the Tanaka and Freed analysis the $R_\perp$ was held fixed for the ordered component independent of mol % of GA.) In our more sophisticated analysis of the present experiments in which we distinguish hydrogen-bonded and non-hydrogen-bonded species and we allow nonlinear least-squares fitting of all parameters, we find $R_\perp$ increases from 4.3×10^6 to 1.15×10^7 and from 2.4×10^5 to $5.0 \times 10^6\ s^{-1}$ for the respective species upon addition of 2 mol % GA at 45°C. (The results for the pure membrane are actually the mean of results for 40° and 52°C.) The nearly isotropic component for 2 mol % GA has an $R_\perp$ nearly equal to that from the ordered hydrogen-bonded species. 5) In both gel and liquid crystal phases, no immobilized component was found. Thus, while we conclude that the effects of GA on the structure and dynamics of lipid membranes aligned by the ISDU and the pressure-annealing are similar, we are able to identify significant differences attributable to the higher water content in the case of the ISDU samples.

We also wish to note that we found it possible to align DPPC membranes containing much higher amounts of GA (i.e., 10 mol %) than could be aligned by pressure-annealing (4 mol %) (results not shown).

Effects of BR

Several lines of evidence indicate that the structural integrity of BR was not significantly affected by the procedure used to incorporate it into the DPPC vesicles, although the proton-pumping photoactivity of BR was not directly measured for this work. As noted above, ultraviolet/visible spectra taken before and after the incubation showed that the protein remained intact during its incorporation into the vesicles. This conclusion is consistent with other studies that have demonstrated that BR maintains its structural integrity even above 65°C. Resonance Raman spectroscopy (Mendelsohn, 1976) has shown that BR retains its photochemical activity at temperatures up to at least 72°C. A DSC study by Jackson and Sturtevant (1978) revealed a reversible transition in the crystalline structure of the membrane between 75°C and 80°C and an irreversible denaturation of the protein at 100°C, both of which were clearly apparent in the ultraviolet/visible spectrum of the membranes. These conclusions have been corroborated by more recent studies of thermal protein unfolding in BR (Cladera et al., 1988; Brouillette et al., 1987).

As pointed out above, there are some noticeable similarities in the effects of GA and BR on the ordering and dynamics of the membranes monitored by spin probe CSL, such as the disordering effect in both the gel and liquid crystal phases and the increase in the rotational mobility in the gel phase. Several important differences between GA and BR are apparent from the ESR results. 1) The disordering effect of BR on the bulk lipid is more dramatic, i.e., a small amount of BR (0.24 mol %) reduces the average order parameter from 0.77 to 0.35 (as monitored by CSL) at 30°C (cf. Table 5), whereas 2 mol % of GA are required to reduce S by a similar factor at 25°C (cf. Table 4). This is presumably due to the much larger size of the BR molecule compared with that of GA. 2) The two-component spectra for BR in aligned membranes persists into the liquid crystal phase, but at present the interpretation of the two components observed in this phase, especially in the lower temperature part of this phase remains uncertain. Such differences between the effects of BR and GA might originate from specificity in the nature of protein/lipid vs. peptide/lipid interactions.

In contrast to the CSL results, only one spectral component is observed in the 16-PC spectra from ISDU-aligned samples containing BR. This observation also contrasts with results on 16-PC in pressure-annealed DPPC membranes containing GA and 3–7 wt % water, in which two-component spectra were clearly observed (Tanaka and Freed, 1985). The absence of a second component in the ISDU sample may reflect differences between lipid/GA interactions versus lipid/BR interactions, or it may simply result from an experimental inability to resolve two components because of the lower ordering of 16-PC at the higher water content (20 wt %) of the ISDU-aligned samples. Nevertheless, addition of BR does slightly reduce the 16-PC order parameter (cf. Results). A more significant conclusion from this observation is that

BR does not significantly immobilize the acyl chain of the boundary lipids. If that were the case, a second broad component should appear in the spectra of the 16-PC label, which is not observed. Instead only a small reduction in $R_\perp$ is obtained from the single component spectrum (cf. Results).

Disaggregation of GA and BR in the gel phase of DPPC

As mentioned above in the discussion of Fig. 8, the broad peak (*a*) in the $\Psi = 0°$ spectrum of CSL in ISDU-aligned DPPC membranes containing 2 mol % GA at 25°C reveals considerably reduced order in the lipids associated with GA. However, when the temperature is increased to around 35°C, (i.e., 15°C below the main gel-to-liquid crystal transition temperature of DPPC), a new peak (*b*) appears concomitant with a decrease in the intensity of peak *a*. This change is reflected in an overall change in the ordering in the membranes, as monitored by $\bar{S}$. Similar line shape changes are observed in the spectra of CSL from the ISDU-aligned DPPC membranes containing 0.24 mol % BR when the temperature is increased from 30°C to 41°C (cf. Fig. 9). Moreover, plots of $\bar{S}$ vs. temperature for both ISDU-aligned samples of GA/DPPC and BR/DPPC systems show a maximum at 50°C and 40°C, respectively (cf. Fig. 7). Dispersion samples of the same composition appear to show modifications in their ESR spectra at these temperatures that correlate with their DSC results but the ESR spectra are more poorly resolved (results not shown). If we compare these ESR results with the DSC measurements, we find that, for both the DPPC/GA and the DPPC/BR systems, the temperatures at which the new ESR peaks appear match the temperature of the broad endothermic DSC peaks (cf. Figs. 12 and 13).

The simulations of the GA/DPPC and BR/DPPC spectra based on the three-component model are able to reproduce the features whereby peak *a* decreases with temperature and peak *b* increases with temperature in the following manner. One finds that peak *a* is mainly due to component 3, the nearly isotropic or disordered component which decreases in population with increase in temperature, especially for GA. Peak *b* for GA is associated with component 2, which manifests itself in the 35° and 45°C spectra of Fig. 8 due to a reduction in its order parameter, and its growth in population between 35° and 45°C. Given the experimental spectral resolution, it was not possible to assign these lower-ordered components to either hydrogen-bonded or non-hydrogen-bonded CSL species.

We are inclined to suggest that the correlation in intensities between the low ordering peak associated with "boundary" lipid and the new peak showing higher ordering, as well as the existence of a maximum in $\bar{S}$ obtained from the simulations of the spectra, reflects a change in structure of the membrane. In attempting to ascribe the nature of this change we are influenced by the following observations. 1) Below T_c of the lipid membrane, BR forms a two-dimensional hexagonal lattice in purple membranes (Henderson, 1975) and in lipid vesicles (Cherry et al., 1978), whereas above T_c, the lattice disaggregates and BR molecules exist in a monomeric state (Cherry et al., 1978). 2) Heyn et al. (1981) suggest in their interpretation of DSC experiments, that the melting process of the lipid/BR membrane associated with the main phase transition (i.e., at T_c) is a solvation of BR molecules by the surrounding lipid molecules. Such a solvation would necessarily imply a structural change sensed by the "boundary" lipids as the BR molecules disaggregate. In this context our ESR results would imply that the lipids associated with the "solvated" or disaggregated BR molecules experience less disordering. 3) Since no pretransition was observed in the DSC experiment for the ISDU-aligned pure DPPC membrane (cf. Fig. 11), the broad endothermic peak in the DSC trace for the ISDU-aligned DPPC/BR sample could reflect an enthalpy change associated with the BR lattice melting and the accompanying BR-lipid solvation process.

In the case of GA, we note that Chapman et al. (1977) have suggested that the peptide molecules segregate from the lipid molecules below T_c. Also, solid state ^{13}C-NMR studies on ^{13}C-labeled GA in chain-perdeuterated DMPC (DMPC-d_{54}) show that well below the T_c of the DMPC-d_{54} GA is immobile, but about 5°C below T_c GA is able to reorient (Cornell et al., 1988a, b). Thus we might expect a disaggregation of GA similar to what we are suggesting for BR.

Although we do not know the details of how the protein/peptide aggregation/disaggregation affects the structure of the lipid membranes, in the DPPC/GA system a progressive increase in the population of the component with nearly isotropic ordering (component 3) from 0 to 0.53, when the temperature is lowered from 50° to 25°C, (cf. Table 4) clearly indicates that the aggregation of the peptide is significantly disrupting the lipid structure.

Thus, our initial results on GA and BR suggest that the ISDU alignment of membranes for spin-label studies in aligned membranes may be useful for resolving subtle effects due to aggregation and dissociation of peptides and integral membrane proteins that might not be observable in dispersion samples.

In addition to the dramatic increase in spectral resolution that is inherent in spin-label studies of aligned membranes, it would be highly desirable to enhance the resolution even further by utilizing recently developed two-dimensional Fourier transform ESR (Gorcester et al., 1989; Freed, 1990; Crepeau et al., 1994) and high-frequency ESR methods, (Budil et al., 1989; Freed, 1990; Earle et al., 1994). These techniques typically require somewhat higher amounts of spin probe than continuous wave methods. Alignment by ISDU should be particularly suitable for such applications, because it provides a means of preparing thicker membrane samples than is available via the pressure-annealing method. We have already had initial success with hydrated ISDU prepared samples studied at 250 GHz (Budil et al., unpublished results).

Aligned lipid bilayers versus membrane dispersions

The ESR results presented above for ISDU-aligned samples containing a peptide or protein differ in some notable respects from ESR studies of unaligned samples. Differences

between samples aligned by pressure-annealing and dispersion samples have been reported previously. Tanaka and Freed (1985) showed that for aligned samples at low water content, addition of GA had only a small effect on the lipid chain motions, and no peaks were seen that are equivalent to those usually ascribed to "trapped" or "immobilized" lipids, which are observed in dispersion samples for larger GA/lipid ratios. Instead they saw in the gel phase that the effect of even small amounts of GA was to disorder the nearby lipid so that the region about the GA no longer preserved the macroscopic alignment of the multilayers. They referred to this region as made up of "boundary" or "disordered" lipids. The results of Tanaka and Freed suggested that "trapped" or "immobilized" lipids could not be supported in the macroscopically aligned model membrane, whereas they could in vesicles. One question of interest in the present study is whether the trends observed for GA in ISDU-aligned vesicles at high water content would more closely resemble the results from pressure-annealed samples at lower water content or those from the vesicle dispersions with excess water.

Ge and Freed (1993) have analyzed ESR spectra from GA/DPPC vesicle dispersions in excess water, and they found that the features of these spectra related to "trapped" or "immobilized" lipids are consistent with boundary lipids for which there is increased ordering but no substantial decrease in mobility except at higher concentration of GA. Thus it would be inappropriate to refer to them as "immobilized" lipids. [Ge and Freed distinguish between disordering due to a decrease in magnitude of the local order parameter from that due to randomization of the direction of alignment. Only the former could be studied in vesicle dispersions, whereas the latter would require aligned samples]. Instead we shall refer to them as "motion-restricted" lipids. We have not studied the regime of high GA (or BR) concentration in the present work on aligned samples to examine whether at higher water content such features could appear.

It should be noted that Ge and Freed (1993) did not have available at that time the newest least-squares algorithms used in the present work that enable fitting several components. Their analysis was more in the spirit of model simulations. That is, they synthesized vesicle dispersion spectra by superposing component spectra that had been selected by a trial-and-error procedure. Only the relative populations of the components were determined by least-squares methods. Also ESR spectra from vesicle dispersions are much less resolved than those from well-aligned samples, and this would necessarily reduce the reliability of full least-squares fitting of such spectra. Thus one may expect that while the principal trends and conclusions discerned by Ge and Freed are appropriate (especially the observation of "trapped lipids" with increased ordering), the fine details are somewhat dependent on the model used.

Ge and Freed (1993) also showed that their analysis applied to lipid vesicles containing large membrane proteins, which also lead to "trapped" lipids with increased ordering. This is consistent with results from studies of BR in dispersion samples, including cell envelope vesicles from *Halobacterium cutirubrum* (Esser and Lanyi, 1973) and DMPC vesicles reconstituted with BR (Rehorek et al., 1985). In both of these studies, an increase in lipid ordering within the vesicles due to BR was reported in the liquid crystal phase. This also contrasts with the present results on BR containing ISDU-aligned samples (cf. Figs. 3 and 7) for which BR reduced the ordering.

Tanaka and Freed (1985) do distinguish two competing effects in the lipid-GA interaction, a disordering feature and a hardening feature as mentioned above. The former is when the presence of GA molecules induces a disordering of the lipids either by reduced ordering or by randomization of the direction of alignment. The latter is when the GA molecules make the membranes more solid, resulting in increased order and decreased rotational rates. They argued that the disordering feature is dominant under conditions of low fluidity, while the hardening feature is dominant when there is high fluidity. Thus we may suggest that the well-aligned ISDU samples, even with appreciable water (20 wt %), are still in the regime characterized by the disordering feature of GA (except at temperatures $\geq$100°C), whereas vesicles in excess water for both GA/DPPC (Ge and Freed, 1993) and BR/DPPC systems (Esser and Lanyi, 1973) are characterized by the hardening feature. This distinction might be due to differences in the molecular packing between multilamellar bilayers and vesicles, (White et al., 1986). The existence of "motion-restricted" lipids in vesicles, but not in oriented bilayers (Tanaka and Freed, 1985) is strong evidence for differences in molecular packing. It is also clear from the work of Tanaka and Freed (1985) that the water content is very important: vesicles in excess water show the hardening feature whereas those with low water content were more consistent with aligned membranes of the same water content in showing the disordering feature.

CONCLUSIONS

We have successfully applied the ISDU method, originally developed by Clark et al. (1980), to ESR spin-label studies on protein-lipid interactions. We have shown that DPPC membranes aligned by ISDU yield reproducible ESR spectra for both the 16-PC and CSL spin probes. The spectra indicate high probe ordering in both gel and liquid crystal phases, comparable to that observed in aligned samples prepared by the pressure-annealing method used in previous spin-label studies.

We have shown that the results from the high water content membranes aligned by ISDU are consistent in their trends with those from the low water content membranes aligned by pressure annealing, even though the high water content membranes exhibit lower ordering and faster diffusional rates.

In the case of GA-containing membranes, a "disordered" component is observed in the gel phase with nearly isotropic order parameters, which is similar to the results of Tanaka and Freed (1985) for low water content. At high water content, however, this disordered component is significantly smaller consistent with the more fluid, less dense membrane being able to accommodate the peptide. In both the gel and liquid

crystalline phases the overall reduction in average order parameter is smaller for the high water content samples. In general the rotational mobility is increased with the addition of GA with the effect being most pronounced for the gel phase.

The study of a BR-containing membrane aligned by ISDU using the CSL probe shows a similar but more dramatic disordering effect, with only 0.24 mol % BR producing a comparable disordered lipid fraction as 2 mol % GA, presumably due to the large molecular size of BR. Addition of BR also increases the rotational mobility of the CSL in the gel phase, but the 0.24 mol % BR has a less dramatic effect than 2 mol % GA.

We have found that between 30° and 40°C, i.e., just below the gel-to-liquid crystal phase transition temperature in ISDU aligned DPPC membranes containing GA or BR, a new component appears with appreciable ordering, as the disordered component is reduced in population. This is correlated in temperature with a broad endothermic peak in the DSC. These observations have tentatively been associated with a structural change of the lipid membranes caused by disaggregation of the GA and BR within the membrane.

The use of the latest nonlinear least-squares algorithms for fitting multicomponent spectra has enabled more reliable interpretation of the results of this study. In particular, we have substantially improved the simulations of ESR spectra of CSL in the gel phase for all the lipid membranes (pure DPPC, GA/DPPC, and BR/DPPC) in terms of a model with both hydrogen-bonded and non-hydrogen-bonded CSL molecules. We find that the CSL molecules hydrogen-bonded to the bilayer interface undergo faster rotational diffusion than those that are not.

The present results and those of Tanaka and Freed (1985), which show a disordered lipid fraction with addition of small amounts of GA or BR in the aligned multilayers, is different from the ESR observations of Ge and Freed (1993) on membrane vesicles in excess water. They found that larger amounts of GA or protein led to "motion restricted" lipids exhibiting an increase in ordering possibly due to differences in molecular packing and water content in these two geometries.

We gratefully acknowledge Prof. A. Scotto of the Cornell Medical School for contributing the BR used in these studies, and Prof. R. Bogomolni of the University of California, Santa Cruz for his kind gift of a culture of *H. cutirubrum*. We wish to thank Dajiang Xu for assistance with some of the initial ESR simulations for this paper and Prof. W. Bryan Lynch for assistance with the ISDU cell design.

This work was supported by National Institutes of Health Grants GM 25862 and RR 07126. D.E.B. acknowledges support from National Institutes of Health NRSA GM 12924. Computations were performed at the Cornell Theory Center and the Cornell Materials Science Center.

REFERENCES

Brouillette, C. G., D. D. Muccio, and T. K. Finney. 1987. pH dependence of bacteriorhodopsin thermal unfolding. *Biochemistry*. 26:7431–7438.

Budil, D. E., K. E. Earle, W. B. Lynch, and J. H. Freed. 1989. Electron paramagnetic resonance at 1 millimeter wavelength. *In* Advanced EPR: Applications in Biology and Biochemistry. A. J. Hoff, editor. Elsevier, Amsterdam. 307–340.

Cadenhead, D. A., and F. Muller-Landau. 1977. Molecular packing in steroid-lecithin monolayers III: mixed films of 3-doxyl-17-androstane with dipalmitoylphosphatidylcholine. *Chem. Phys. Lipids*. 25:329–343.

Casadio, R., and W. Stoeckenius. 1980. Effect of protein-protein interactions on light adaptation of bacteriorhodopsin. *Biochemistry*. 19:3374–3381.

Chapman, D., B. A. Cornell, A. W. Ellasz, and A. Perry. 1977. Interactions of helical polypeptide segments which span the hydrocarbon region of lipid bilayers. Studies of the gramicidin A lipid-water system. *J. Mol. Biol.* 113:517–538.

Cherry, R. J., U. Muller, R. Henderson, and M. P. Heyn. 1978. Temperature-dependent aggregation of bacteriorhodopsin in dipalmitoyl- and dimyristoylphosphatidylcholine vesicles. *J. Mol. Biol.* 121:283–298.

Cladera, J., M. L. Galisteo, M. Dunach, P. L. Mateo, and E. Padros. 1988. Thermal denaturation of deionized and native purple membranes. *Biochim. Biophys. Acta*. 943:148–156.

Clark, N. A., and K. J. Rothschild, 1982. Preparation of oriented multilamellar arrays of natural and artificial biological membranes. *In* Methods in Enzymology, Vol. 88. 326–333.

Clark, N. A., K. J. Rothschild, D. A. Luppold, and B. A. Simon. 1980. Surface-induced lamellar orientation of multilayer membrane array. *Biophys. J.* 31:65–96.

Cornell, B. A., F. Separovic, A. J. Baldassi, and R. Smith. 1988a. Conformation and orientation of gramicidin A in oriented phospholipid bilayers measured by solid state carbon-13 NMR. *Biophys. J.* 53:67–76.

Cornell, B. A., L. E. Wier, and F. Separovic. 1988b. The effect of gramicidin A on phospholipid bilayers. *Eur. Biophys. J.* 16:113–119.

Crepeau, R. H., S. Rananavare, and J. H. Freed. 1987. Automated least-squares fitting of slow motional ESR spectra. Abstracts of 11th International EPR Symposium, Rocky Mountain Conference, Denver, CO.

Crepeau, R. H., S. Saxena, S. Lee, B. Patyal, and J. H. Freed. 1994. Studies on lipid membranes by two-dimensional Fourier transform ESR: enhancement of resolution to ordering and dynamics. *Biophys. J.* 66: 1489–1504.

De Kruijff, B., R. A. Demel, and L. L. M. Van Deenen. 1972. The effect of cholesterol and epicholesterol incorporation on the permeability and on the phase transition of intact Acholeplasma laidlawii cell membranes and derived liposomes. *Biochim. Biophys. Acta*. 255:331–347.

Demel, R. A., K. R. Bruckdorfer, and L. L. M. Van Deenen. 1972. Structural requirements of sterols for the interaction with lecithin at the air-water interface. *Biochim. Biophys. Acta*. 255:311–320.

Dennis, J. E. J., and R. B. Schnabel. 1983. Numerical Methods for Unconstrained Optimization and Nonlinear Equations. Prentice-Hall, Englewood Cliffs, NJ.

Dongarra, J. J., C. B. Moler, J. R. Bunch, and G. W. Stewart. 1979. Linpack Users' Guide. Society for Industrial and Applied Mathematics, Philadelphia.

Earle, K. A, J. K. Moscicki, M. Ge, D. E. Budil, and J. H. Freed. 1994. 250 GHz-ESR studies of polarity gradients along the aliphatic chains in phospholipid membranes. *Biophys. J.* 66:1213–1221.

Esser, A. F., and J. K. Lanyi. 1973. Structure of the lipid phase in cell envelope vesicles from *Halobacterium cutirubrum*. *Biochemistry*. 12:1933–1939.

Forbes, J., J. Bowers, X. Shan, L. Moran, E. Oldfield, and M. A. Moscarelle. 1988. Some new developments in solid-state nuclear magnetic resonance spectroscopic studies of lipids and biological membranes, including the effects of cholesterol in model and natural systems. *J. Chem. Soc. Faraday Trans. I*. 84:3821–3849.

Frank, H. A., R. Friesner, J. A. Nairn, G. C. Dismukes, and K. Sauer. 1979. The orientation of the primary donor in bacterial photosynthesis. *Biochim. Biophys. Acta*. 547:484–501

Freed, J. H. 1990. The Bruker lecture: modern techniques in EPR spectroscopy. *J. Chem. Soc. Faraday Trans.* 86:3173–3180.

Ge, M., D. E. Budil, and J. H. Freed. 1994. An electron spin resonance study of interactions between phosphatidylcholine and phosphatidylserine in oriented membranes. *Biophys. J.* 66:1515–1521.

Ge, Mingtao, and J. H. Freed. 1993. An electron spin resonance study of interactions between gramicidin A′ and phosphatidylcholine bilayers. *Biophys. J.* 65:2106–2123.

Gorcester, J., G. L. Millhauser, and J. H. Freed. 1989. Two dimensional and Fourier transform EPR. *In* Advanced EPR: Applications in Biology and Biochemistry. A. J. Hoff, editor. Elsevier, Amsterdam. 177–242.

Griffith, O. H., P. J. Dehlinger, and S. P. Van. 1974. Shape of the hydrophobic barrier of phospholipid bilayers (evidence for water penetration in biological membranes). *J. Membrane Biol.* 15:159–192.

Henderson, R. 1975. The structure of the purple membrane from Halobacterium halobium: analysis of the x-ray diffraction pattern. *J. Mol. Biol.* 93:123–138.

Herbette, L., J. Marquardt, A. Scarpa, and J. K. Blasie. 1977. A direct analysis of lamellar x-ray diffraction from hydrated multilayers of fully functional sarcoplasmic reticulum. *Biophys. J.* 20:245–252.

Heyn M. P., A. Blume, M. Rehorek, and N. A. Dencher. 1981. Calorimetric and fluorescence depolarization studies on the lipid phase transition of bacteriorhodopsin-dimyristoyl-phosphatidylcholine vesicles. *Biochemistry.* 20:7109–7115.

Hubbell, W. L., and H. M. McConnell, 1971., Molecular motion in spin-labeled phospholipids and membranes. *J. Am. Chem. Soc.* 93:314–326.

Jackson, M. B., and J. M. Sturtevant. 1978. Phase transition of the purple membranes of Halobacterium halobium. *Biochemistry.* 17:911–915.

Jost, P. C., O. H. Griffith, R. A. Capaldi, and G. Vanderkooi, 1973a. Evidence for boundary lipid in membranes. *Proc. Natl. Acad. Sci. USA.* 70:480–484.

Jost, P. C., O. H. Griffith, R. A. Capaldi, and G. Vanderkooi. 1973b. Identification and extent of fluid bilayer regions in membranous cytochrome oxidase. *Biochim. Biophys. Acta.* 311:141–152.

Kar, L., E. Ney-Igner, and J. H. Freed, 1985. Electron spin resonance and electron-spin- echo study of oriented multilayers of L_α-dipalmitoylphosphatidylcholine water system. *Biophys. J.* 48:569–595.

Keough, K. M., E. Oldfield, and D. Chapman, 1973. Carbon-13 and proton nuclear magnetic resonance of unsonicated model and mitochondrial membranes. *Chem. Phys. Lipids.* 10:37–50.

Koole, P., A. J. Dammers, and Y. K. Levine. 1984. Q-band electron spin resonance studies of slow motion in bilayers with high order. *Chem. Phys. Lipids.* 35:161–174.

Lee, D. C., A. A. Durrani, and D. Chapman. 1984. A difference infrared spectroscopic study of gramicidin A, alamethicin and bacteriorhodopsin in perdeuterated dimyristoylphosphatidylcholine. *Biochim. Biophys. Acta.* 769:9–56.

Marsh, D., 1980. Molecular motion in phospholipid bilayers in the gel phase: long axis rotation. *Biochemistry.* 19:1632–1637.

Marsh, D., and A. Watts, 1981. Spin labeling and lipid-protein interactions in membranes. *In* Lipid-protein Interactions, Vol. 2. P. C. Jost and O. H. Griffith, editors. John Wiley, New York. 53–126.

Meirovitch, E., and J. H. Freed. 1984. Analysis of slow-motional electron spin resonance spectra in smectic phase in terms of molecular configuration, intermolecular interactions, and dynamics. *J. Phys. Chem.* 88: 4995–5004.

Meirovitch, E., D. Igner, G. Moro, and J. H. Freed. 1982. Electron-spin relaxation and ordering in smectic and supercooled nematic liquid crystals. *J. Chem. Phys.* 77:3915–3938.

Meirovitch, E., A. Nayeem, and J. H. Freed. 1984. Analysis of protein-lipid interactions based on model simulations of electron spin resonance spectra. *J. Phys. Chem.* 88:3454–3465.

Mendelsohn, R. 1976. Thermal denaturation and photochemistry of bacteriorhodopsin from halobacterium cutirubrum as monitored by resonance Raman spectroscopy. *Biochim. Biophys. Acta.* 427:295–301.

More, J. J., B. S. Garbow, and K. E. Hilstron. 1980. User's Guide for MINPACK-1. National Technical Information Service, Springfield, VA.

Powers, L., and N. A. Clark. 1975. Preparation of large monodomain phospholipid bilayer smectic liquid crystals. *Proc. Natl. Acad. Sci. USA.* 72: 840–843.

Powers, L., and P. S. Pershan. 1977. Monodomain samples of dipalmitoylphosphatidylcholine with varying concentrations of water and other ingredients. *Biophys. J.* 20:137–151.

Rehorek, M., N. A. Dencher, and M. P. Heyn. 1985. Long-range lipid-protein interactions. Evidence from time-resolved fluorescence depolarization and energy-transfer experiments with bacteriorhodopsin-dimyristoylphosphatidylcholine vesicles. *Biochemistry.* 24:5980–5988.

Rice, D., and E. Oldfield. 1979. Deuterium nuclear magnetic resonance studies of interactions between dimyristoylphosphatidylcholine and gramicidin A. *Biochemistry.* 18:3272–3279.

Rothschild, K. J., and N. A. Clark. 1980. Polarized infrared spectroscopy of oriented purple membrane. *Biophys. J.* 25:473–488.

Rothschild, K. J., K. M. Rosen, and N. A. Clark. 1980. Incorporation of photoreceptor membrane into a multilamellar film. *Biophys. J.* 31:45–52.

Sankaram, M. B., and T. H. Thompson. 1991. Cholesterol-induced fluid-phase immiscibility in membranes. *Proc. Natl. Acad. Sci. USA.* 88: 8686–8690.

Schneider, D. J, and J. H. Freed. 1989. Calculating slow motional magnetic resonance spectra: a user's guide. *In* Spin Labeling Theory and Applications, Vol. 8. L. J. Berliner and J. Reuben, editors. Plenum Press, New York. 1–76.

Seber, G. A. F., and C. J. Wild. 1989. Nonlinear Regression. John Wiley, New York.

Shimoyama, Y., L. E. Goran Eriksson, and A. Ehrenberg. 1978. Molecular motion and order in oriented lipid multilayer membranes evaluated by simulations of spin label ESR spectra. *Biochim. Biophys. Acta.* 508:213–235.

Shin, Y.-K., D. E. Budil, and J. H. Freed. 1993. Thermodynamics and dynamics of phosphatidylcholine-cholesterol mixed model membranes in the liquid crystalline state. *Biophys. J.* 65:1283–1294.

Shin, Y.-K., and J. H. Freed. 1989a. Dynamic imaging of lateral diffusion by electron spin resonance and study of rotational dynamics in model membranes. *Biophys. J.* 55:537–550.

Shin, Y.-K., and J. H. Freed. 1989b. Thermodynamics of phosphatidylcholine-cholesterol mixed model membranes in the liquid crystalline state studied by the orientational order parameter. *Biophys. J.* 56:1093–1100.

Silvius J. R., and P. M. Brown. 1986. Role of head group structure in the phase behavior of amino phospholipid. Hydrated and dehydrated lamellar phases of saturated phosphatidylethanolamine analogue. *Biochemistry.* 25:4249–4258.

Tanaka, H., and J. H. Freed. 1984. Electron spin resonance studies on ordering and rotational diffusion in oriented phosphatidylcholine multilayers: evidence for a new chain-ordering transition. *J. Phys. Chem.* 88: 6633–6643.

Tanaka, H., and J. H. Freed. 1985. Electron spin resonance studies of lipid-gramicidin interactions utilizing oriented multibilayers. *J. Phys. Chem.* 89:350–360.

Vanderkooi, G. 1994. Computation of mixed phosphatidylcholine-cholesterol bilayer structures by energy minimization. *Biophys. J.* 86: 1457–1468.

Vogel H., F. Jahnig, V. Hoffmann, and J. Stumpel. 1983. The orientation of melittin in lipid membranes, a polarized infrared spectroscopy study. *Biochim. Biophys. Acta.* 733:201–209.

White S. H., R. E. Jacobs, and G. I. King. 1986. Molecular packing differences in liposomes and oriented lipid multilayers. *Biophys. J.* 49:435a.

Williams, B. W., A. W. Scotto, and C. D. Stubbs. 1990. Effect of proteins on fluorophore lifetime heterogeneity in lipid bilayers. *Biochemistry.* 29: 3248–3255.

Wong, P. T. T., S. E. Capes, and H. H. Mautsch. 1989. Hydrogen bonding between anhydrous cholesterol and phosphatidylcholines: an infrared spectroscopic study. *Biochim. Biophys. Acta.* 980:37–41.